

## Response to reviewers

We thank the three anonymous reviewers for their excellent and insightful feedback on the manuscript. The most significant changes made to the manuscript at this stage include providing more detail in the descriptions of the piston and pressure stabilization system as well as the water traps and adding a section that discusses the current sample requirements. In the following we address specific comments individually.

### Anonymous Referee #1

L24 Why presumably? Are there other possible causes e.g. discussed in the 7 papers cited here?

We thank the reviewer for pointing out this ambiguity. We rephrased the sentence to focus on the lack of direct observational evidence instead. Helium isotope studies have placed some constraint on an atmospheric  $^3\text{He}/^4\text{He}$  trend but are limited by analytical uncertainty and uncertainty about the stability of  $^3\text{He}$  in the atmosphere ( e.g., Boucher et al., 2018). Evidence from helium isotope studies is discussed in more detail later in the manuscript.

L34  $^{14}\text{C}$  is neither a trace nor a greenhouse gas.

Yes, we changed the phrasing to “societally-important greenhouse gases and geochemical tracers such as [...]” in order to encompass  $^{14}\text{C}$ .

L42-44 This is correct for the tracers listed here, but not for more recently introduced ones in e.g. Leedham Elvidge et al., ACP, 2018. Also, as stratospheric air can be several years old, these gases are governed by their respective tropospheric growth rates and its variability over time (and so is the  $\text{He}/\text{N}_2$  ratio).

We thank the reviewer for bringing up this issue. New tracers of stratospheric age of air are needed as exemplified by the work of Leedham Elvidge et al., (2018). We hope that  $\text{He}/\text{N}_2$  may become one of several new tracers that will become a useful tool to study stratospheric circulation because each tracer is characterized by a unique set of advantages and limitations. We modified the paragraph to also mention the role of the tropospheric increase of  $\text{He}/\text{N}_2$ .

L50 Isn't this limit dependent on the amount of air used?

In theory, the use of very large air samples could improve the precision of  $^3\text{He}/^4\text{He}$  measurements. However, in practice the use of static vacuum mass spectrometers places important limits on sample size.

L53 This should probably be just Boucher et al., 2018c.

Yes, we corrected the text.

L82 Please cite Fuller et al. properly.

We clarified that we are citing a method presented by Reid et al. (1987).

L96 Does "the level of roughly  $\pm 30$  per meg per year" describe the analytical precisions or the actual trend? Also, consider splitting this very long sentence into two.

Observed trends of atmospheric  $^3\text{He}/^4\text{He}$  in recent studies are scattered near zero and have an uncertainty of about 30 per meg. We have split the sentence and clarified the language.

L110 This should be "on the order of" or perhaps "below" (considering Table 1, where estimates in the  $10^8$  range are listed). Do these estimates include the impact of large volcanic eruptions?

We corrected the typo. Note that the estimate refers to moles of  $\text{N}_2$ . Due to the large abundance of  $\text{N}_2$  in the atmosphere, only changes at the level of  $10^{14}$  mol  $\text{y}^{-1}$  or greater would have a significant impact on  $^4\text{He}/\text{N}_2$ . Volcanic emissions, even from large volcanic eruptions, are unlikely to reach that level.

L124 "Fig. 2C" creates the impression that the figure consists of several separate sub-figures which is not the case. Consider rephrasing e.g. to "C in Fig. 2".

Thank you for pointing this out. We adopted the proposed phrasing.

L124-126 It's not clear to me from this description a) how the pistons move the tubing, b) how stress to the tubing moving outside the chamber is dealt with and c) how often this part of the system develops leaks (or whether this has been checked at all). See also my comment on the caption of Fig. 2.

We thank the reviewer for this important question and have provided more detail about the pistons and the stabilization chamber in the text. We also modified Fig. 2 to show a more detailed schematic of the sliding seal setup to address this issue. Note that the sliding tubing does not need to make a high-vacuum seal because pressure in the stabilization chamber is only varied between 6-16 psi and actively maintained. The sliding seal (as all aspects of the setup) were screened for leakage by spraying pure He around potential weak points and we have never experienced any leakage.

L130 Please specify which vacuum grease is used.

We added the information to the manuscript.

L131 Why does the outlet capillary have to be thermally insulated? What is the required temperature stability? Also, to which diameter has the capillary been crimped and why?

Changes in temperature lead to changes in conductance of the capillary. Temperature fluctuations could therefore erode the air flow stabilization. Temperature fluctuations at the crimp have not been quantified but empirically, the addition of more thermal mass to the crimped tubing has improved the stability of the  $^4\text{He}$  beam. The capillary diameter has also been established empirically. The degree of crimping was chosen to yield the maximum air flow that could be safely accepted by the mass spectrometer without risking frequent arcing due to excessive pressure in the MS source.

L134 Please quantify "high purity".

We added the information to the manuscript.

L145-146 Which criteria are used to judge whether the Ti needs replacing? What are the volume and dimensions of the getter oven and how is it heated?

We agree with the reviewer that this is important information and have added it to the text under section 2.2. Ti is replaced when the gettering capacity is exhausted and  $\text{N}_2$  begins to break through as can be monitored from an increase in MS source pressure.

L152-154 How is a "complete flush-out" ensured? What is the internal volume of the flushed-out parts? Shouldn't the getter oven be flushed for longer since the flow in there breaks down by a factor of ~100?

Flush-out time is determined by the pressure and volume flow of gas through our inlet and determined empirically. The flush-out time is equivalent to the switching response time scale of inlet system seen in Fig. 5. After removal of O<sub>2</sub> and N<sub>2</sub> in the getter, the volume flow is roughly 100x smaller, but pressure drops simultaneously ensuring that the purging time of the getter is comparable to the tubing upstream. The empirically determined flush-out time is consistent with the volumes and flows seen in the system. We have changed the phrasing in the text to shift the focus of the reader towards the time scale of returning to a constant MS signal after switching, which is the ultimate goal. Furthermore, we clarified the importance of the pressure drop in the getter oven.

L171 How does one adjust the crimping of the capillaries, especially without risking to break them?

Stainless steel capillary tubing is squeezed between two pieces of aluminum: a flat piece and a dowel. Crimping can be adjusted by adjusting two screws which hold the pieces of aluminum together. Relaxing the force applied allows the capillary tubing to spring back. If necessary, the relaxation can be assisted manually with pliers by gently squeezing the tubing at a 90 degree angle to the direction of the crimping force.

L165-166 At which temperature?

Cylinders are stored at room temperature in the thermal enclosure. We added this information to the text.

L166-167 That sounds dangerous. How is compliance with Health and Safety regulations ensured?

Capillaries and fittings are made from metal and are rated for high pressure applications. Even in the unlikely case of a failure of the capillary tubing, gas could only escape at very low flow due to the small diameter of the capillary tubing. Therefore, the operation is inherently safe.

L171-173 What is the nature of this cold trap and how is its temperature stability ensured? What is its internal volume and how often does it need cleaning/exchanging? What mechanisms are in place to prevent ice building up in the vicinity?

The water trap is cooled by a mixture of dry ice and ethanol. Small changes in temperature are inconsequential as flows from the sample and standard are stabilized later before reaching the MS. The tubing is removed from the dry ice and ethanol mixture after each analysis while dry air flow through the tubing continues. This allows any residual water in the trap to be carried away with the gas stream and any ice build-up on the tubing to melt.

L186 Have any other cycle times been tested?

The cycle time was chosen to ensure complete signal stabilization after switching as determined by evaluating information in Fig. 5. No additional times were tested.

L203-205 If the uncertainty of the correction is 6 per meg, why does it increase the analytical uncertainty by only 2 per meg? Also, what about the uncertainty of 1.5 h measurements?

Uncertainties are added in quadrature here and  $\sqrt{8^2+6^2}=10$ . By a similar expression, uncertainty of 1.5h measurements would increase to 16 per meg. No changes were made to the manuscript.

L211-213 What are the uncertainties of the corrections?

We thank the reviewer for this question. We added a sentence explaining that “Analytical uncertainty for measurements of  $\delta(\text{O}_2/\text{N}_2)$ ,  $\delta(\text{Ar}/\text{N}_2)$ , and  $dX_{\text{CO}_2}$  is typically better than 1.5 per meg, 11 per meg, and 0.2 ppm (Keeling et al., 1998, 2004), yielding uncertainties of 0.3, 0.11 and 0.2 per meg in the terms  $\delta\left(\frac{\text{O}_2}{\text{N}_2}\right)X_{\text{O}_2}$ ,  $\delta(\text{Ar}/\text{N}_2)X_{\text{Ar}}$ , and  $dX_{\text{CO}_2}$ ”

L216 I’m not sure that the derivation of this relationship should be part of a Discussion section as it’s rather a methodological part of the manuscript. Also, how much larger than relative changes in N<sub>2</sub> are relative changes in CO<sub>2</sub>?

Seasonal changes in atmospheric N<sub>2</sub> due to dissolution in the ocean are on the order of a few per meg. Changes in CO<sub>2</sub>, in contrast, are currently around 2.5 ppm per year or around 6000 per meg. We have moved the derivation into methods and given it its own section.

L217-265 This section focuses on the multitude of possibilities that the new technique might enable, but fails to draw much attention to its limitations (e.g. the large amount of air required, which is not easily acquired from the stratosphere, or the long analysis times, which will limit constraints on spatial gradients in volcanic plumes or near oil or gas facilities).

We thank the reviewer for this suggestion and added a paragraph at the end of the discussion section that summarizes important limitations of our measurement system. Efforts are ongoing to address these limitations, lessen sample size and pressure requirements, and to reduce the duration of individual measurements.

L235 Do the authors perhaps mean “possible complications that affect <sup>3</sup>He measurements” here?

A potential problem for estimating a <sup>4</sup>He source from <sup>3</sup>He/<sup>4</sup>He is that <sup>3</sup>He emissions from different sources such as tritium decay could bias estimates of the <sup>4</sup>He source. We changed the text to make this clearer.

L273 2x “avoids the need”

The second “avoids the need” was removed.

L278-282 I’m not sure that it’s necessary to list all these references again. It certainly doesn’t help the readability.

Thank you! We removed the references as they are extensively covered in the introduction.

L451-453 Very little detail is provided (in both the figure and the caption) on how the piston system looks and operates. Since this is a crucial part of the inlet system I urge the authors to expand their explanation and perhaps include a cross-section of this chamber. Also, how does the pneumatic control work?

We thank the reviewer for raising this issue. We added more detail to the text and figure on the pistons and pressure stabilization system (see answer to related comment above).

L477 How many sigmas?

1 sigma. We included the information in the caption.

L490 Table 1 has a lot of empty space and at the same time an enormous amount of footnotes, which make it rather difficult to follow. Consider reorganising, e.g. through naming the references in the table or moving some of the explanations into the caption. Also, what uncertainty range is connected to the assumption of  $^3\text{He}/^4\text{He} = 3\text{e-}8$ ?

We reformatted the table to improve space usage. We have not considered uncertainty about  $^3\text{He}/^4\text{He}$  of fossil fuels because the uncertainty about the actual  $^3\text{He}/^4\text{He}$  trend dominates. The estimate of  $^3\text{He}/^4\text{He} = 3\text{e-}8$  is based on Sano et al (2013).

## Anonymous Referee #2

\* The measurement yields the mole fraction of He in the sample gas matrix, normalized relative to the He mole fraction in a gas standard. However, the method is presented in the manuscript to yield the (absolute?) He/N<sub>2</sub> ratio of the sample. This is rather confusing, as N<sub>2</sub> is NOT part of the measurement (in fact, N<sub>2</sub> is removed from the gas sample before MS analysis). The conversion of the measurement result (He mole fraction) to the He/N<sub>2</sub> ratio is based on a simple mathematical manipulation and some assumptions about the composition of the gas matrix. This conversion seems trivial and is not related to the measurement technique; and I don't see the need for it. I suggest to avoid this confusion by removing He/N<sub>2</sub> (or He/O<sub>2</sub> etc.) as far as possible (from the title and most of the text), and to focus on the true nature of the measurement, i.e., on the (relative) He mole fraction.

We decided to frame the manuscript in terms of He/N<sub>2</sub> rather than the helium mole fraction because He/N<sub>2</sub> is more readily interpretable in terms of distinct physical processes than the helium mole fraction. Measurements of the helium mole fraction are influenced by both changes in helium and changes in any other component of air. Anthropogenic activity has already led to dramatic changes in the composition of our atmosphere and these changes would obscure the signals from processes that are unique to helium. Because an important contribution of the paper is to develop potential scientific applications of the helium mole fraction measurement, we believe the current framing of the manuscript best serves this purpose. However, we agree that it is critical to clearly distinguish between the helium mole fraction, i.e. the quantity actually measured, and He/N<sub>2</sub>. To this end, we have altered the title and abstract of the manuscript to avoid confusion.

\* The manuscript is missing a review/overview of existing techniques for He analysis in air (3He/4He, He/Ne, He mixing ratio). Without this background, it is difficult to understand on what grounds the new method was designed, and how it improves on previous methods, both in terms of instrumental techniques and scientific applications. The manuscript should be revised to better develop the link of the new method to existing techniques. What were the design targets for the new instrument? What was the design approach to achieve these targets? Why was the new method implemented in this way?

We thank the reviewer for these suggestions. A high precision <sup>4</sup>He/N<sub>2</sub> measurement has never been attempted before and opens new fields of research. We added a brief explanation of the analytical technique used for helium isotope analysis, and an additional paragraph discussing measurements of the helium mixing ratio. The manuscript in its current form already describes the inherent limitations of the helium isotope method and outlines advantages of a <sup>4</sup>He/N<sub>2</sub> measurement (lines 45--53). The lack of analytical precision in the helium isotope measurement was a key motivation for developing the <sup>4</sup>He/N<sub>2</sub> measurement. Potential scientific applications enabled by the new measurement technique are discussed in detail in the introduction of the manuscript as well as the discussion section. We believe a discussion of He/Ne would mostly distract from the main aims and application of the paper.

\* As it is, I am not convinced about the scientific utility of the new method: (1) Earlier work with static MS systems for He isotope analysis showed that their 0.2% precision was sufficient to resolve the expected atmospheric He variations (for example: Mabry et al, EPSL, 2015). Why exactly is a new method with approx. 100x better precision required to study the evolution of the atmospheric He?

Recent studies using helium isotopes to constrain trends in atmospheric helium abundance have found no significant trend (Lupton and Evans, 2013; Mabry et al., 2015; Boucher et al., 2018). This is contradicted

by theoretical predictions of a  $^4\text{He}$  build-up in bottom-up approaches (e.g., Oliver et al., 1984; Pierson-Wickmann et al., 2001). A likely explanation for this conundrum is that the anthropogenic signal is too small to be detected with the current analytical precision, which motivates work to improve atmospheric helium measurements. Moreover, atmospheric helium changes in the stratosphere and troposphere from gravitational fractionation are similarly undetectable with current methods, providing a compelling impetus to develop new analytical method.

(2) Most publications on atmospheric He acknowledged that the quality of the historic/archived air samples put major limitations on the uncertainty of reconstructing the atmospheric He abundance (for an overview see for example: Brennwald et al, EPSL, 2013 / reference missing in the manuscript). Further improving the instrumental precision of the He analysis does not help with this fundamental issue. I am therefore not convinced that an improvement of the instrumental precision is very useful to study some of the effects noted by the authors.

Cylinders containing archived air dating back to 1974 are available at Scripps Institution of Oceanography. Similar cylinders are routinely used as standard cylinders for  $\text{O}_2/\text{N}_2$  and  $\text{Ar}/\text{N}_2$  analysis. These cylinders have shown very limited drift over 20 years (Keeling et al., 2007) suggesting that under the right circumstances, archived air should provide a faithful record of atmospheric helium changes over the last 4 decades. Note that Brennwald et al (2013) is not cited in the manuscript as it has been superseded by Mabry et al. (2015)

(3) With an analysis time of 6-8 hours and a sample gas consumption of 28 mL per minute, a single analysis requires about 10-14 L of sample gas. However, typical samples of historic/archived air are typically in the order of 0.1-100 mL (see refs. cited in the manuscript, and as given above), which is 2 to 5 orders of magnitude too low for the new method described in the manuscript. The large gas consumption of the new method therefore severely limits the technical applicability to large-volume gas archives, which are scarce and may not be readily available for consumption to a (destructive!) analysis.

The reviewer raises an important limitation of the analysis method. This and other limitations are now discussed in a separate discussion section. The need for samples of 10-14l is however not prohibitive as the aforementioned high-pressure cylinders still contain about 3000 l (STP) of old air.

In order to illustrate the scientific potential of the new method, the manuscript should be extended with application examples targeted at the scientific questions described in the introduction. I suggest to add a few measurements of real world historic/archived air samples to demonstrate the true utility and suitability of the new method to study the He change due to fossil fuel extraction (and analogous for stratospheric circulation).

Real world measurements of archived air will be presented in a separate paper. To illustrate the fidelity of the measurement, we would like to instead point the reviewer to Cylinder A shown in Fig. 6. Cylinder A was filled in 2008 and is compared to air pumped in 2019 on the same pumping system. The two cylinders indeed demonstrates an increase in  $^4\text{He}$  by about 700-800 per meg over 11 years.

\* What is the purpose of the cold traps at the gas inlet system? My guess is that they are meant to remove water vapor from the sample/standard gas streams, but I am not sure. This should be described better.

That is correct and was clarified in the text.

\* The intensity of the He ion beam in the MS is controlled by the sample/standard gas flow to the gas inlet system. As far as I can tell, the precision of the analysis result is therefore controlled crucially by the inlet system, and in particular by the cold traps and the pressure regulators: (1) Cold traps: the efficiency of the water removal from the gas streams is likely not stable over time, and will therefore introduce a variation of the He mixing ratio in the gases. How can the cold trap variation be avoided such the He mixing ratio in the gas stream is stable to 10 per meg or better?

We thank the reviewer for this question. The mole fraction measured is defined on a dry air basis, so removal of water is mandatory and does not result in a bias, by definition. The stability of the mass flow to the getter oven and MS is indeed critical to the integrity of the measurement. The mass flow stability is ensured by the combined stability of the thermally insulated crimp and the actively controlled pressure in the stabilization chamber. Any pressure changes caused upstream for example at the water traps are cancelled out. At -80C, the water vapor content of air drops to less than 1 ppm. Even if there were small changes in trap temperature, we would therefore expect these to be  $\ll$  1ppm and hence not significantly impact the helium mole fraction measurement. Note that we do not use regulators but crimped capillaries to regulate flow from high pressure cylinders to ensure metal seals throughout the system.

(2) The gas pressure at the main capillary inlet directly controls the gas flow into the capillary, and hence the He flow into the MS. Similarly to the cold traps, this seems to imply that the pressure at the capillary inlet must be stabilized to 10 per meg or better. How is this technically possible? I don't have a strong background with large-volume dynamic MS gas analysis, so I may be overlooking something that may be obvious to the authors (I am mostly into static and low-volume dynamic MS). However, I believe it would be very difficult to achieve such tight stability controls over the gas inlet system, and there must be some way to avoid or compensate such variations in the gas inlet in order to achieve the 10 per meg precision in the He mixing ratio of the gas sample. I feel these points need to be explained better.

We appreciate the reviewer's question and expanded the discussion of the stabilization chamber and the sliding tubing in the manuscript. During operation, the pressure in the stabilization chamber is held constant at 96.5 kPa to within about 0.0133322 Pa. This corresponds to a stability of 0.14 per meg. Such precise pressure control is made possible by differential pressure gauges, which achieve a resolution of 1/10000 of their full range (full range is 0.2 Torr on our gauge).

\* Title: "Measurements of ..." seems to indicate that the focus of the paper is to present new measurement data. I'd suggest to change focus to the new analysis method / technique.

We thank the reviewer for the suggestion changed the title to "A method for resolving changes in atmospheric He/N<sub>2</sub> as an indicator of fossil fuel extraction and stratospheric circulation".

\* Line 26/27: "...gases heavier than air in the stratosphere..." → what gases other than air are in the stratosphere? Also, does the gravitational separation only apply to heavier gases, not lighter ones?

Gases heavier than air such as argon are depleted in the stratosphere due to gravitational separation while gases lighter than air such as helium are enriched by the same process. We changed the language of the text to clarify this.

\* Line 56/57: I'd assume that N<sub>2</sub> and other "noble" gases are seasonally variable due to atmosphere/ocean gas exchange, which is subject to the temperature dependence of N<sub>2</sub> solubility in the water (e.g., Keeling et al., Tellus 322–338, 2004). Note that the He solubility dependence on temperature is much less than

for N<sub>2</sub>. While this effect may be relatively small, it should at least be noted in the text (if the N<sub>2</sub> normalization is not removed entirely, see above).

The role of ocean heat exchange is indeed small. This is discussed in a full paragraph in the manuscript (lines 102-107).

\* Line 83: Using the equations given above, I calculate  $\delta(\text{He}/\text{N}_2) = -6.4$ , not 7.5 (note the sign!). Please check.

We thank the reviewer for this question. Inserting all the terms in the equation, we get a gravitational fractionation signal that is 7.5 times greater and of opposite sign for He/N<sub>2</sub> than for Ar/N<sub>2</sub>. We clarified this important point in the text. Note that the diffusivities used are for the gases in air, not in a binary mixture.

\* Line 95: "...no significant trend in atmospheric <sup>3</sup>He/<sup>4</sup>He has been observed..." → there are many different studies with different (and sometimes contradicting!) conclusions regarding the existence and size of the atmospheric <sup>3</sup>He/<sup>4</sup>He change. Considering the work cited in the manuscript it seems wrong to say "no significant trend was observed", and this argument needs to be revised. To this end, it might be useful to take a look at Brennwald et al, EPSL, 2013, which has a compilation and comparison of different studies on the atmospheric <sup>3</sup>He/<sup>4</sup>He change, and also presents some measurements on He changes observed in archived air samples.

The full sentence this quote is taken from is "However, in contrast to these predictions and some earlier observations (Oliver et al., 1984; Sano et al., 1989, 2010; Pierson-Wickmann et al., 2001), no significant trend in atmospheric <sup>3</sup>He/<sup>4</sup>He has been observed using archived air samples spanning from the beginning of the 20<sup>th</sup> century to today." It is correct that observations by Sano et al. suggested a trend in atmospheric helium isotopes. This has been disputed by several other studies (e.g., Lupton and Graham, 1991; Lupton and Evans, 2004, 2013; Mabry et al., 2015; Boucher et al., 2018). Of particular significance here is that all 3 studies of direct air samples published in the last 8 years did not find any significant trend. The analysis of Brennwald et al. (2013) was repeated and corrected by Mabry et al. (2015) and is therefore not included in this list. We believe our phrasing adequately reflects the disagreement about observed trends of <sup>3</sup>He/<sup>4</sup>He and appropriately emphasizes recent results.

\* Line 144: "...compared to the 30-second switching timescale." → what does this refer to? Switching of what?

This refers to the timescale of switching between sample and standard gas in the inlet system. We clarified the wording in the text.

\* Line 156: "Background concentrations..." → what "background" is this? "Blank"? "Residual"? m/z=4 signal with analysis of He free gas? Or with the inlet to the MS closed? Please define.

The background is determined with the inlet closed upstream of the getter oven, but all other aspects of the analytical system in their normal measurement mode (e.g. high voltage ion acceleration and magnetic field strength appropriate for <sup>4</sup>He analysis, etc). We modified the manuscript accordingly.

\* Line 172: The geometry of the cold trap crucially controls the operation and performance of the cold trap. Is this a U shaped tube? Or a 'washing flask' type? Or something else? Please explain the details of the cold traps ("made from 1/4" stainless steel" is not sufficient).

We are grateful for this excellent question and have added more details to the description of the (U-shaped) trap system.

\* Line 175–178: Why is the performance of the getter important (as long as it is not "dead" and works as a pump to draw the air matrix into the capillary)? As far as I can tell, the He flow rate into the MS is identical to the He flow rate into the getter. I therefore don't see how the getter can affect the He analysis (as long as the getter operation is stable between the analysis runs of the sample and standard gases). How does the getter affect the performance of the He analysis? Does the getter performance affect the He analysis at all? Please explain.

An effective removal of N<sub>2</sub> and O<sub>2</sub> is important to reduce competition with He for electrons in the gas mixture that reaches the MS source. This ensures a brighter He<sup>+</sup> beam. We added a sentence to clarify this. It is also important to avoid introducing too much gas into the MS because too high pressures will lead to source instability and ultimately a failure of the instrument.

\* Line 201: What does "the 5% level" refer to? Is this a statistical "significance level"? What kind of statistics? Please explain.

This refers to the weighted multiple linear regression analysis described in the text. We changed the phrasing of the manuscript to make this more apparent.

\* Fig. 7 shows the measured zero effect, with a substantial scatter (about +/- 50 per meg or so). However, the discussion in the main text indicates a zero-effect uncertainty of only 6 per meg. I am confused because I don't understand how the +/- 50 per meg scatter is consistent with the 6 per meg uncertainty. I believe my confusion is due to some ambiguity in how the zero-effect is quantified and compensated during the analysis and data processing routines. This should be explained better.

We thank the reviewer for this question. Lines 197-202 describe the results of a weighted multiple linear regression analysis of the zero-enrichment test. Uncertainties and statistical significance are products of this established statistical method. We improved the phrasing of the paragraph to explain this better.

\* Tab. 2: what is the meaning of "scaled" Xe peak heights? What kind of "scaling" was applied, and how? Please explain.

Xe was not directly observable due to limitations of the dynamic range of a MAT 253 configured to measure He. The MAT 253 has two different magnet ranges, only one of which enables He measurements, and it is prohibitively time consuming to switch between ranges during a mass scan. Instead we report expected Xe peak heights based on previous knowledge about the relative ion yield of Kr and Xe from an air sample. The manuscript was clarified.

### Anonymous Referee #3

I think the analytical precisions of mass spectrometry can be classified into “internal precision”, “internal reproducibility” and “external reproducibility” (see Bender et al., 1994, *Geochim. Cosmochim. Acta.*). Internal precision indicates a standard error of  $xx$  cycles in a 1-block analysis, and internal reproducibility indicates a standard deviation of the repeated analyses of several blocks. I think the authors did not distinguish between internal precision and internal reproducibility in the paper, and the presented internal precision of  $\pm 15$  per meg for sample run of 1.5h and  $\pm 8$  per meg over 6h (line 186-187) are standard error ( $1\sigma/\sqrt{n}$ ),  $n$  = number of the total cycles  $\sim$  about 1,800 and 7,200 for 1.5h and 6h, respectively). The internal precision is shown as error bars in Fig. 6, and the variability of every cycle measurements is presented in Fig. 3 (b) (the unit “per meg” is needed for the y-axis label of Fig. 3 (b)). I hope I have not misunderstood or misinterpreted the presentation.

We thank the reviewer for this suggestion. We have clarified the distinction between the standard error of cycles (here called internal precision) and the standard deviation of repeat analyses (here called external reproducibility) in the manuscript. We now described the nature of the error bar in figure captions. We also corrected the y-axis label of Fig. 3 (b).

2) Fig. 6 shows  $d(\text{He}/\text{M})$  values of 8 (5) times repeated analyses of the 6-8h measurements of Cylinder A (B) against La Jolla air. I think it corresponds to the external reproducibility in the context of Bender et al., but I have some concerns: Is the La Jolla air identical to the “He/N<sub>2</sub> reference material (line 163-165)”, “standard gas cylinder (line 188)”, and “reference (Fig. 2)”? Please clarify to avoid confusion. Assuming that the standard and La Jolla air are identical and used as the reference in Fig. 2, how do the authors ensure the short-to-long term stability of the La Jolla air? In other words, how long does it take to obtain the results of 8 or 5 times repeated measurements shown in Fig. 6? If it takes several days, then I agree that the stability of the standard is enough for the period, however, future work is needed to confirm much longer-term stability for the observations of seasonal and interannual variations in the atmospheric He/N<sub>2</sub> ratio.

A high-pressure cylinder containing La Jolla air collected in 2019 has served as the reference gas for this work. The short-term stability of this standard against another high-pressure cylinder is demonstrated in Figure 6. Data for this Figure was collected over a roughly 2-week period. Future work is needed to evaluate the long-term stability of the analysis system as outlined by the reviewer and discussed in the manuscript. We have revised the naming of the reference gas and made it consistent throughout the paper.

3) Please provide information related to the needed minimum and maximum inner pressures of the sample and reference gas to maintain the appropriate flow rate of 27-28 mL/min using capillary. In this regard, I sort of remember Scripps flask samples being collected at an atmospheric pressure. If so, I don't think these flasks can be used for the He/N<sub>2</sub> analysis, as described in the present study. How do the authors collect pressurized air samples without significant fractionation of He and N<sub>2</sub>?

The pressure downstream of the water traps and upstream of the pressure stabilization chamber is roughly 3 atm to allow sufficient flow into the chamber when the chamber is kept at 96.9 kPa. The reviewer is correct that Scripps O<sub>2</sub> and CO<sub>2</sub> flasks are collected at atmospheric pressure, and the new method we describe here does not involve the Scripps O<sub>2</sub> and CO<sub>2</sub> flasks. The pressurized samples used

here are pumped with a heavy-duty compressor and fractionation is largely avoided by the quantitative capture of a very large amount of air (~3000 liters) in a short time with minimal leakage.

Some changes will be needed to use Scripps O<sub>2</sub> network flask directly as samples. Compatibility might be achievable by simultaneously (i) dropping the pressure in the stabilization chamber, (ii) adjusting the flow restriction after the stabilization chamber to offset the reduction in flow to the MS, and (iii) increasing the conductance of tubing delivering gas into the chamber. None of these changes should present a major obstacle and work is ongoing to accommodate flask samples. In the meantime, the system can accept pressurized air samples including a suite of high-pressure cylinders available at SIO that contain air sampled over the last 40 years. Acceptable agreement in O<sub>2</sub>/N<sub>2</sub> and Ar/N<sub>2</sub> between flask samples and high-pressure cylinders routinely filled at SIO suggests they might be suitable to reconstruct atmospheric changes in He/N<sub>2</sub>. Results from these cylinders will be presented in a future publication.

4) Related to the comment 3) above, there does not seem to be any discussion of the analyses of the locally pumped ambient air shown in Fig. 2. I would be very much interested in hearing from the authors some information regarding the ambient air analyses, since it will serve as an indicative evaluation of “true” external reproducibility, including air sampling procedures, such as inlet fractionation, and leakage or permeation of He through pump diaphragm.

The measurement system was initially setup for analysis of ambient air but unfortunately never deployed because of limited instrument time. We removed it from the text and diagram as there is no data available to evaluate performance.

5) I think the response of d(He/N<sub>2</sub>) measured by the mass spectrometer to the actual H<sub>2</sub>/N<sub>2</sub> ratio of a sample air will likely be linear, but some checks are needed. Please provide some concrete evidence to that effect.

We thank the reviewer for this question. On the MAT 253, ion beams are reported in voltages rather than currents for technical reasons. The ion beam current in counts per second (I) is related to the voltage (V) read by the resistance (R) according to Ohms’ law:  $I(\text{Cps}) = V/R$

The manufacturer’s instrument specifications state that nonlinearity of the MAT253 mass spectrometer for CO<sub>2</sub> isotopes is better than 0.06 per mille per 1 Volt change in the ion beam when introducing pure CO<sub>2</sub> into the MS. The <sup>4</sup>He beam is collected on a 10<sup>12</sup>Ω resistor and roughly yields a voltage of 1.5V. The largest <sup>4</sup>He beam strength difference between sample and standard that we expect to measure is about 3 per mille or 0.0045V. If the <sup>4</sup>He beam behaved like CO<sub>2</sub> isotopes in the MS the nonlinearity bias would be 4.5×0.06=0.00027 per mille.

However, a leading cause for non-linearity in a MS are changes in total source pressure, which are minimal in our application. As the gas mixture that enters the MS source consists mostly of Ar and atmospheric Ar concentrations are stable to within a few per meg, we expect the MS response in our application to be absolutely linear.

6) The potential application of He/N<sub>2</sub> to evaluate interannual variability in the stratospheric circulation (±375 per meg/yr, expected value) is very interesting and is an excellent idea, considering that it can provide better signal-to-noise ratio than Ar/N<sub>2</sub>. In order to extract the gravitational fractionation signal of He/N<sub>2</sub>, it is necessary to subtract the He/N<sub>2</sub> change due to chemical processes such as fossil fuel extraction (which yields 35 – 350 per meg/yr of secular He/N<sub>2</sub> trend at the surface) from the observational

results in the stratosphere. I guess the authors have plans to observe surface He/N<sub>2</sub> variations, so that a precise secular trend in the troposphere will be achieved in the near future. However, as reported by Engel et al. (2009 Nature Geoscience), CO<sub>2</sub> or SF<sub>6</sub> age of the stratospheric air samples show interannual variability by about ±1 years. This interannual variability of the age corresponds to ±35 – ±350 per meg of the stratospheric He/N<sub>2</sub> change due to the fossil fuel extraction, if we ignore attenuation of the interannual variability from the surface to the stratosphere. Therefore, to evaluate the interannual variability in the stratospheric circulation based on gravitational fractionation of He/N<sub>2</sub>, precise determination of He/N<sub>2</sub> age will be important. However, as Ray et al. (2017 JGR) and Sugawara et al. (2018 ACP) reported, CO<sub>2</sub> age and SF<sub>6</sub> age do not necessarily agree with each other. Given these issues, I would be very much interested in hearing how the authors are planning to determine the age of He/N<sub>2</sub>.

We thank the reviewer for the excellent question. As explained by the reviewer, a correction for the tropospheric trend will be needed for the calculation of age of air (AoA) from stratospheric helium measurements. Furthermore, a fundamental relationship between gravitational fractionation of He/N<sub>2</sub> and AoA in the stratosphere will need to be determined. This could be done for example by building on previous modelling work by Birner et al. (2020). The atmospheric transport model TOMCAT has been validated for the relationship between Ar/N<sub>2</sub> and AoA in the lower stratosphere and results for He/N<sub>2</sub> could be obtained by a simple scaling or implementation of He as a new tracer in the model. These modeling results would establish a He/N<sub>2</sub>-AoA relationship that would be valid in the absence of any tropospheric He/N<sub>2</sub> trend. However, a correction for any potential tropospheric helium variability would be needed to apply this calibration to real data. Depending on the complexity of the tropospheric helium variability, different approaches are potentially feasibility. In the simplest and most likely case of a linear (or at least near-linear) increase of tropospheric He/N<sub>2</sub>, the He/N<sub>2</sub>-AoA relationship could be modified by subtracting the linear He/N<sub>2</sub> change. In the case of a more complex tropospheric history, the tropospheric record would have to be convolved with an assumed age spectrum to obtain an appropriate correction. This is possible but will rely on assumptions about the shape of the age spectrum. We believe this goes beyond the scope of the paper and is therefore not addressed in the text.

7) Line 198: “9 psi, 14 psi, and 16 psi. . .” should be changed to “9, 14, and 16 psi”.

The repeated usage of the unit was removed.

8) Line 202: “-9.61±7.2 per meg, 1±3.7 per meg, and -15.7 per meg. . .” should be changed to “-9.61±7.2, 1±3.7, and -15.7 per meg. . .”.

The repeated usage of the unit was removed.

9) References: Please change “2” in CO<sub>2</sub>, O<sub>2</sub>/N<sub>2</sub>, Ar/N<sub>2</sub> and SF<sub>6</sub> to subscripts.

We thank the reviewer for catching this oversight. We implemented correct usage of subscripts in the reference section.

# Measurements of atmospheric $^4\text{He}/\text{N}_2$ as an indicator of fossil fuel extraction and stratospheric circulation

Benjamin Birner<sup>1</sup>, William Paplawsky<sup>1</sup>, Jeffrey Severinghaus<sup>1</sup>, and Ralph F. Keeling<sup>1</sup>

<sup>1</sup> Scripps Institution of Oceanography, UC San Diego, La Jolla, CA 92093, USA

Correspondence to: Benjamin Birner (bbirner@ucsd.edu)

**Abstract.** The atmospheric  $\text{He}/\text{N}_2$  ratio is expected to be increasing due to the emission of He associated with fossil fuels and is expected to also vary in both space and time due to gravitational separation in the stratosphere. These signals may be useful indicators of fossil-fuel exploitation and variability in stratospheric circulation, but direct measurements of  $\text{He}/\text{N}_2$  ratio are lacking on all time scales. Here we present a high-precision custom inlet system for mass spectrometers that continuously stabilizes the flow of gas during sample-standard comparison and removes all non-noble gases from the gas stream. ~~This, enabling-enables~~ unprecedented accuracy in measurement of relative changes in the helium mole fraction, which in the can be directly related to the  $^4\text{He}/\text{N}_2$  ratio using supplementary measurements of  $\text{O}_2/\text{N}_2$ ,  $\text{Ar}/\text{N}_2$  and  $\text{CO}_2$ . Repeat measurements of the same combination of high-pressure tanks using our inlet system achieves a  $\text{He}/\text{N}_2$  reproducibility of  $\sim 10$  per meg (i.e. 0.001%) in 6–8h analyses. This compares to interannual changes of  ~~$\text{He}/\text{N}_2$~~ -gravitational enrichment at  $\sim 35$  km in the mid latitude stratosphere of order 300–400 per meg, and an annual tropospheric increase from human fossil fuel activity of less than  $\sim 30$  per meg  $\text{y}^{-1}$  (bounded by previous work on helium isotopes). The gettering and flow-stabilizing inlet may also be used for the analysis of other noble gas isotopes and could resolve previously unobserved seasonal cycles in  $\text{Kr}/\text{N}_2$  and  $\text{Xe}/\text{N}_2$ .

## 1 Introduction

The atmospheric mole fraction of helium in dry air is typical  $\sim 5.24$  ppm (Glückauf, 1944) with an isotopic abundance of  $^4\text{He}$  about  $10^6$  times greater than  $^3\text{He}$ . On geological time scales, the natural concentration of  $^4\text{He}$  in the atmosphere is set by a balance of  $^4\text{He}$  loss to space and  $^4\text{He}$  release from the Earth's crust, where it is produced by radioactive decay of uranium and thorium (Kockarts, 1973; Pierson-Wickmann et al., 2001; Sano et al., 2013; Torgersen, 1989; Zartman et al., 1961). Over the past century, human exploitation of fossil fuels likely has accelerated the release of crustal He (Boucher et al., 2018c; Lupton and Evans, 2013, 2004; Mabry et al., 2015; Oliver et al., 1984; Pierson-Wickmann et al., 2001; Sano et al., 1989), but ~~direct observations the observational evidence~~ of a secular increase of atmospheric  $^4\text{He}$  ~~are lacking-remains ambiguous presumably due to a lack of analytical precision~~ (Boucher et al., 2018c; Lupton and Evans, 2013, 2004; Mabry et al., 2015; Oliver et al., 1984; Pierson-Wickmann et al., 2001; Sano et al., 1989). Additionally, recent measurements and model simulations reveal a

30 small depletion of ~~heavy gas argon gases heavier than air~~ in the stratosphere by gravitational separation (Belikov et al., 2019; Birner et al., 2020; Ishidoya et al., 2020, 2018, 2013, 2008; Sugawara et al., 2018) suggesting a corresponding enrichment of the light gas helium. Gravitational separation is only partially counteracted by the large-scale stratospheric circulation and mixing, which tends to homogenize the atmosphere. Variability in stratospheric circulation and stratosphere-troposphere exchange (STE) could therefore impact the degree of fractionation and cause additional interannual changes in the stratospheric  
35 and, to a much lesser extent, the tropospheric abundance of  $^4\text{He}$ .

Measurements of  $\text{He}/\text{N}_2$  may provide an alternative indicator of variations in stratospheric circulation and STE. An improved understanding of STE is critical because stratospheric circulation changes affect tropospheric trends of societally-important ~~trace and~~ greenhouse gases and geochemical tracers such as  $\text{N}_2\text{O}$ ,  $\text{CH}_4$ ,  $^{14}\text{C}$ ,  $\text{O}_3$  and CFCs (Arblaster et al., 2014; Graven et al., 2012; Hamilton and Fan, 2000; Hegglin and Shepherd, 2009; Montzka et al., 2018; Nevison et al., 2011; Simmonds et al.,  
40 2013). These gases all have significant sources or sinks in the stratosphere that cause strong stratosphere-troposphere concentration differences. Global circulation models consistently predict an acceleration of the stratospheric Brewer-Dobson Circulation (BDC; Brewer, 1949; Dobson, 1956) under global warming (Butchart, 2014). Stratospheric circulation is also naturally modulated on a range of shorter time scales from synoptic-scale events to decadal variations (e.g., Holton et al., 1995; Li et al., 2012; Flury et al., 2013; Butchart, 2014; Ray et al., 2014). Circulation changes have typically been observed using  
45 measurements of numerous different trace gases in the stratosphere (e.g.,  $\text{CO}_2$ ,  $\text{SF}_6$ ,  $\text{H}_2\text{O}$ ,  $\text{O}_3$ ,  $\text{CO}$ , or  $\text{N}_2\text{O}$ ) (e.g., Bönisch et al., 2009; Engel et al., 2009, 2017; Ray et al., 2010; Haenel et al., 2015). However, interpretation of these tracers of stratospheric circulation is complicated by complex chemical sources and sinks processes and tropospheric histories, whereas gravitational fractionation of  $\text{He}/\text{N}_2$  is governed by comparatively simple physics and expected to increase smoothly in the troposphere.

50 Atmospheric  $\text{He}/\text{N}_2$  measurements may also provide an indication of the history of fossil-fuel usage. Previous attempts to measure the fossil-fuel signal in He ~~has have~~ centered on measurements of changes in the atmospheric  $^3\text{He}/^4\text{He}$  isotope ratio typically using multicollector, static vacuum mass spectrometers (Boucher et al., 2018c; Lupton and Evans, 2013, 2004; Mabry et al., 2015; Oliver et al., 1984; Sano et al., 1989). However, measurements of the  $^3\text{He}/^4\text{He}$  ratio are fundamentally limited by the extremely low abundance of  $^3\text{He}$  (e.g., Mabry et al., 2015; Boucher et al., 2018b), with only about 1 in 730,000 He atoms  
55 being  $^3\text{He}$ . Therefore, the precision on individual  $^3\text{He}/^4\text{He}$  analyses is currently limited to  $\sim\pm 0.2\%$  ( $2\sigma$ ). This is insufficient for the detection of the stratospheric and anthropogenic signals we are interested in, and which we estimate to cause variations in the atmospheric  $^4\text{He}$  ~~mole fraction~~abundance on the order of 0.0030 to 0.04%  $\text{y}^{-1}$  (see section 2.1 & 2.2.). Moreover, small changes in  $^3\text{He}$  from radioactive decay of tritium in nuclear warheads may complicate the interpretation of  $^3\text{He}/^4\text{He}$  results (e.g., ~~Christine~~-Boucher et al., 2018c; Lupton and Evans, 2004).

60 Thus far, the most promising direct measurements of the atmospheric  $^4\text{He}$  mixing ratio were produced by Holland and Emerson (1987). Holland and Emerson repeatedly introduced sample and standard air into a mass spectrometer through a charcoal trap to concentrate helium. However, their method also only achieved an instrument precision of 0.22% ( $2\sigma$ ) and is thus not suitable for the science discussed above.

Here we describe a method to measure relative differences in  $^4\text{He}$  mole fraction ( $^4\text{He}/\text{M}$ ) between two large samples of air using a custom mass spectrometer inlet system. The helium mole fraction can later be mathematically translated to our target ratio,  $^4\text{He}/\text{N}_2$ , given supplementary measurements of  $\text{O}_2$ ,  $\text{Ar}$ , and  $\text{CO}_2$  (see discussion). This is advantageous because  $\text{N}_2$  is near-constant in the atmosphere making  $^4\text{He}/\text{N}_2$  more readily interpretable than  $^4\text{He}/\text{M}$ . The  $^4\text{He}/\text{M}$  method depends on stabilization of the ~~gas-air~~ flow to the ion source between a sample and standard gas to achieve high precision differencing. Novel elements in our setup include continuous flow removal of reactive gases via titanium gettering immediately upstream of the mass spectrometer inlet, and the use of an actively-controlled open split (Henneberg et al., 1975) for balancing pressures upstream of a shared capillary directed towards the mass spectrometer. Gas handling techniques, the inlet system and the continuous-flow getter oven are described in detail below.

### 1.1 Gravitational fractionation of $\text{He}/\text{N}_2$ in the stratosphere

The notion that the stratospheric and tropospheric  $\text{He}/\text{N}_2$  ratio must vary in response to fluctuations in stratospheric circulation is based on studies of the atmospheric  $\text{Ar}/\text{N}_2$  ratio (Birner et al., 2020; Ishidoya et al., 2020). Relative changes in the  $\text{Ar}/\text{N}_2$  ratio (or  $\text{He}/\text{N}_2$ ) are commonly expressed in delta notation:

$$\delta(\text{Ar}/\text{N}_2) = \frac{\left(\frac{\text{Ar}}{\text{N}_2}\right)_{SA}}{\left(\frac{\text{Ar}}{\text{N}_2}\right)_{ST}} - 1 \quad (1)$$

where subscripts SA and ST refer to the ratio in a sample and a ~~reference-standard~~ gas mixture, respectively.  $\delta(\text{Ar}/\text{N}_2)$  is multiplied by  $10^6$  and expressed in “per meg” units.

Sensitivity tests with the 2-D chemical-dynamical-radiative model of the atmosphere SOCRATES by Ishidoya et al. (2020) indicate that significant temporal changes in stratospheric  $\text{Ar}/\text{N}_2$  should occur in response to an acceleration or deceleration of the BDC. The simulations also suggest a weak stratospheric influence on tropospheric  $\text{Ar}/\text{N}_2$ . Ishidoya et al find that imposing a gradual acceleration of the BDC of  $4\% \text{ dec}^{-1}$  leads to a 40 per meg  $\text{dec}^{-1}$  increase in  $\delta(\text{Ar}/\text{N}_2)$  at  $\sim 35$  km altitude in northern mid-latitudes, and a corresponding 1.3 per meg  $\text{dec}^{-1}$  decrease of  $\delta(\text{Ar}/\text{N}_2)$  in the troposphere. Furthermore, they find that imposing 3-year periodic changes of 10% in BDC yields anomalies of  $\pm 25$  and  $\pm 0.4$  per meg in stratospheric and tropospheric  $\delta(\text{Ar}/\text{N}_2)$ , respectively. Tropospheric observations of  $\delta(\text{Ar}/\text{N}_2)$  by Ishidoya et al. (2020) would be consistent with larger STE-induced interannual changes of tropospheric  $\text{Ar}/\text{N}_2$ . Variability of the BDC on the order of 10% or more on seasonal to decadal time scales is consistent with published estimates (Flury et al., 2013; Ray et al., 2014; Salby and Callaghan, 2006).

The atmospheric  $\text{He}/\text{N}_2$  ratio must be more strongly impacted by gravitational fractionation than  $\text{Ar}/\text{N}_2$  due to the larger mass difference and higher diffusivity of He than Ar, which brings He closer to gravitational equilibrium. The gravitational fractionation effect on  $\text{He}/\text{N}_2$  can be scaled from  $\text{Ar}/\text{N}_2$  (Birner et al., 2020) using the molar mass difference to air  $\Delta M_i$  ( $\Delta M_i = M_i - 0.02896 \text{ kg mol}^{-1}$ ) and the molecular diffusivity  $D_i$  of gas  $i$  in air as:

$$\delta\left(\frac{\text{He}}{\text{N}_2}\right) = \frac{\left(\frac{\text{He}}{\text{N}_2}\right)_{SA}}{\left(\frac{\text{He}}{\text{N}_2}\right)_{ST}} - 1 \approx \frac{D_{\text{He}}^{\text{air}} \Delta M_{\text{He}} - D_{\text{N}_2}^{\text{air}} \Delta M_{\text{N}_2}}{D_{\text{Ar}}^{\text{air}} \Delta M_{\text{Ar}} - D_{\text{N}_2}^{\text{air}} \Delta M_{\text{N}_2}} \delta(\text{Ar}/\text{N}_2). \quad (2)$$

Using the method of Fuller et al. as reported in Fuller method (Reid et al., 1987),  $D_{\text{He}}^{\text{air}}/D_{\text{He}}^{\text{He}}$  is 3.6 (3.5) times greater than  $D_{\text{Ar}}^{\text{air}}/D_{\text{Ar}}^{\text{Ar}}$  ( $D_{\text{N}_2}^{\text{air}}$ ), and  $\Delta M_{\text{He}}/\Delta M$  is more than twice as large and opposite sign than  $\Delta M_{\text{Ar}}$  ( $\Delta M_{\text{He}} = -0.02496$ ,  $\Delta M_{\text{Ar}} = 0.01102$ ,  $\Delta M_{\text{N}_2} = -0.0009466$ ). This makes, making  $\delta(\text{He}/\text{N}_2) \sim -7.5$  times more strongly fractionated by gravity than  $\delta(\text{Ar}/\text{N}_2)$  in the stratosphere but in opposite direction.

## 1.2 Other controls on tropospheric He/N<sub>2</sub>

A variety of known natural processes influence tropospheric <sup>4</sup>He/N<sub>2</sub> is summarized in Figure 1 and Table 1. Natural <sup>4</sup>He release from the Earth's crust is mediated by volcanism, ground water discharge and diffusive leakage. At the same time, helium is lost to space by thermal and non-thermal escape (Kockarts, 1973; Oliver et al., 1984; Pierson-Wickmann et al., 2001; Sano et al., 2013; Torgersen, 1989). Based on these natural fluxes and the total atmospheric burden, the atmospheric residence time of <sup>4</sup>He is estimated to be ~1 million years.

Over the few last centuries, He release from fossil-fuel extraction has dwarfed the natural release rates of <sup>4</sup>He by several orders of magnitude. Based on knowledge of fossil fuel usage and He content of the material (Table 1) the additional <sup>4</sup>He release rate is estimated to be of order 3 to 30×10<sup>10</sup> mole yr<sup>-1</sup> (e.g., Oliver et al., 1984; Sano et al., 1989, 2013; Pierson-Wickmann et al., 2001) implying that <sup>3</sup>He/<sup>4</sup>He should be decreasing at rates between 35 and 350 per meg y<sup>-1</sup>. However, in contrast to these predictions and some earlier observations (Oliver et al., 1984; Pierson-Wickmann et al., 2001; Sano et al., 2010, 1989), no significant trend in atmospheric <sup>3</sup>He/<sup>4</sup>He has been observed using archived air samples spanning from the beginning of the 20<sup>th</sup> century to today. These more recent observations bound any trend in <sup>3</sup>He/<sup>4</sup>He to within -at the level of- roughly ±30 per meg per year (2σ), suggesting similarly small increase rates in  $\delta(\text{He}/\text{N}_2)$  (Boucher et al., 2018c; Lupton and Evans, 2013, 2004; Mabry et al., 2015).

He release from fossil-fuel extraction is also expected to impose an interhemispheric gradient in  $\delta(\text{He}/\text{N}_2)$ . A rough upper bound can be estimated by assuming all fossil-fuel derived He emissions occur in the Northern Hemisphere and interhemispheric mixing of the atmosphere has a time scale of about one year. This would yield a north-south difference of 30 per meg, equal to the expected annual rise in  $\delta(\text{He}/\text{N}_2)$ .

Seasonal and long-term ocean warming can cause small changes in He/N<sub>2</sub>, mainly due to the impact on N<sub>2</sub>. From observations of  $\delta(\text{Ar}/\text{N}_2)$  (Keeling et al., 2004) and solubility data of Ar, He and N<sub>2</sub> (Hamme and Emerson, 2004; Weiss, 1971), we estimate that the impact on He/N<sub>2</sub> of air-sea exchanges is on the order of 0.16 per meg y<sup>-1</sup> for the secular ocean warming trend and 3-9 per meg for seasonal heat exchanges. Therefore, the ratio of stratospheric signals to ocean warming is ~12 times greater for He/N<sub>2</sub> than Ar/N<sub>2</sub> and the effect of slow ocean warming is over two orders of magnitude smaller than the influence of fossil fuel exploitation.

The He/N<sub>2</sub> ratio could also be impacted by processes changing atmospheric N<sub>2</sub>. However, the annual removal of 7.5x10<sup>12</sup> moles N<sub>2</sub> y<sup>-1</sup> by anthropogenic nitrogen fixation in agriculture, combustion, and industry is clearly negligible compared to the ~1.4x10<sup>20</sup> moles of N<sub>2</sub> in the whole atmosphere (Fowler et al., 2013). Volcanic emissions of N<sub>2</sub> are likewise negligible, on the order of 10<sup>9</sup> moles y<sup>-1</sup>.

## 125 2 Methods

Our He/N<sub>2</sub> analysis method relies on measuring the helium mole fraction relative difference between an air sample and a standard ~~reference~~-gas using a single collector for <sup>4</sup>He<sup>+</sup> on a magnetic sector mass spectrometer (MS). Crucially, whole dry air is pressure-stabilized to a high level prior to getting, so that the beam intensity ratio being measured is effectively the <sup>4</sup>He to air ratio. Measurements of the He mole fraction difference can also be expressed similarly to Eq. (1) as  $\delta(^4\text{He}/M)$  where M is  
130 total moles. By applying small corrections for variations in O<sub>2</sub>/N<sub>2</sub>, Ar/N<sub>2</sub>, and CO<sub>2</sub>, the quantity  $\delta(^4\text{He}/M)$  is easily related to  $\delta(^4\text{He}/\text{N}_2)$ .

The MS is interfaced to a custom inlet system with on-line getting and active flow stabilization using an actively pressure-controlled open split (Henneberg et al., 1975), as shown in Figure 2.

### 2.1 The Inlet system

135 The design of the inlet system incorporates elements of an open split (Henneberg et al., 1975) but further stabilizes the pressure using active control elements and allows active switching between a sample (SA) and reference standard gas stream (ST). Pneumatically-actuated pistons (B in Fig. 2E) alternately slide 0.3-mm tubes exhausting sample or standard gas close to a shared intake capillary which is placed at the end of the stabilization chamber (C in Fig. 2D) and connects the chamber to the getter oven and MS. Air actuation of the pistons is controlled by the MS through an electronic valve assembly (Clippard, model: EMS-08). The flexible 0.3mm tubes are mounted leak-tight inside sturdier 1/16" OD tubing which is fixed to the piston and moved with a stroke length of 7 cm. A sliding seal is made between 1/8" OD outer tubing and the 1/16" OD tubing using a compressed O-ring lubricated with TorrLube vacuum grease. This setup creates a movable feedthrough port for the 0.3-mm tubes containing sample and standard gas and the pressure stabilization chamber, thus allowing the chamber to be operated at a selected pressure above or below ambient. The default setting is 14 psia (96.5 kPa).The chamber is shaped as a funnel to  
145 guide the sliding tubing into a reproducible resting position. Variations in chamber pressure are measured with a 0.2-Torr MKS 223B differential pressure gauge and are limited to better than 1 part in 10<sup>6</sup> by opening an MKS Type 248 Control Valve, which allows most of the gas in the stabilization chamber to be pumped away by a vacuum pump. The valve is controlled via an MKS 250E Control Module. ~~The 0.3mm tubes enter the chamber through sliding seals lubricated with vacuum grease, thus allowing the chamber to be operated at a selected pressure above or below ambient. The default setting is 14 psia (96.5 kPa).~~  
150 The shared outlet capillary from the pressure-stabilization chamber is crimped and thermally insulated to avoid changes in

~~conductance and thus air flow caused by room temperature fluctuations.~~ The pressure in the getter oven (~~D in Fig. 2E~~) is about 2 mTorr (0.3 Pa) because the getter material effectively acts as a vacuum pump.

## 2.2 Continuous-flow gettering

In the getter chamber (~~D in Fig. 2E~~), ~~high-purity~~99.9% pure titanium sponge (Ti) irreversibly reacts with N<sub>2</sub>, O<sub>2</sub>, CO<sub>2</sub>, and other non-noble gases in air to form titanium nitride (TiN), titanium dioxide (TiO<sub>2</sub>), titanium carbide (TiC) and other compounds at ~850°C. This increases the concentration of He in the gas mixture by a factor of about 100, boosting precision. The getter oven ~~has an inner diameter of 0.94 cm and a length of 22.5 cm.~~ It is manufactured from heat resistant stainless steel (SS310) and equipped with VCR face seals for easy maintenance. The temperature of the getter oven is determined by manually adjusting the power provided to ~~two OMEGA CRWS semi-cylindrical heaters~~ ~~the furnace~~ surrounding the getter. The ~~furnace heaters~~ ~~is~~are additionally equipped with an independent limit controller for safety.

The gettering efficiency depends on the ~~furnace's~~ heaters' temperature and must be balanced against material tolerance and increased evolution of H<sub>2</sub> gas from the metal in the getter. H<sub>2</sub> forms a solid solution in Ti and is continuously released to the gas stream when Ti is heated. The solution process is reversible and H<sub>2</sub> is absorbed if the Ti is cooled down. H<sub>2</sub> could interact with He<sup>+</sup> in the source or combine with ionized gas to form hydride compounds such as ArH<sup>+</sup> (Fig. 3) However, since the H<sub>2</sub> flux into the gas stream varies slowly compared to the 30-second ~~switching~~ timescale of switching between sample and standard gas, the impact of H<sup>+</sup> cancels during sample-standard comparison. In its current size (~10–12 g Ti), the getter can be used for 70–80-h before the Ti must be replaced to prevent N<sub>2</sub> breakthrough. This requires breaking vacuum in the inlet approximately once every four weeks depending on usage. After replacement, fresh titanium is gradually heated to 900°C over ~12h in isolation from the MS to allow degassing without contaminating the MS. A coarse mesh of metal wire and 2-μm SWAGELOK filters on both sides of the getter prevent getter-derived dust from entering the vacuum system and MS.

## 2.3 Inlet operation

We have developed customized scripts using the software ISODAT provided with any MAT253 mass spectrometer to control the inlet system and operate the pneumatic actuators for He/M analysis (Fig. 3). In a typical run, the instrument performs sample-standard gas switching with a ~30 second switching time (~60 sec full cycle), using a conservative 18-second idle time to ~~ensure complete flush out of the stabilization chamber and the getter oven~~ allowing the MS signal to stabilize before integration. As customary in dynamic MS noble gas application, we group each analysis into blocks consisting of (i) adjusting the accelerating voltage to find the center of the <sup>4</sup>He peak followed by (ii) 20 sample-standard comparisons. Background concentrations of <sup>4</sup>He in the MS are determined daily by closing the inlet upstream of the getter oven and subtracted daily. Data are quality controlled and anomalous cycles are rejected when delta values deviate by more than 3 standard deviations from the smoothed time series or when there are abrupt changes detected in the ion beam associated with instability in the MS source (not shown). ISODAT also monitors the MS source pressure and closes the external change-over-valve (Fig. 2) to protect the MS in case of a pressure control failure.

## 2.4 Gas handling and sample delivery systems

185 Air ~~can is be~~ delivered to the inlet system from ~~either~~ a pair of high-pressure gas cylinders (~~A in Fig. 2A~~) ~~or from a continuous-~~  
~~flow system (Fig. 2B) pumping locally sampled ambient air directly to the laboratory.~~ For He/N<sub>2</sub> ~~reference material~~ standard  
gas, we rely on compressed dry air stored in ~~high-high~~ pressure cylinders, as is conventional for atmospheric measurements of  
O<sub>2</sub>/N<sub>2</sub>, CO<sub>2</sub>, and Ar/N<sub>2</sub> (Keeling et al., 2007). All cylinders are stored horizontally for 2 days in a thermal enclosure at ambient  
temperature before analysis to minimize the risk of thermal fractionation. The pressure is dropped to slightly above ambient  
190 directly at the head valve of high-pressure cylinders using capillaries rather than regulators. The use of capillaries ensures that  
all wetted parts are exclusively metal, which is impermeable to He, and eliminates problems we encountered using regulators  
during initial tests. Due to the use of capillaries, the gas delivery system cannot be evacuated efficiently and instead must be  
purged for several hours ahead of analysis until the signal stabilizes. The flow rates in the lines are monitored using 0.1 liter  
per minute ~~0.11~~ Omron DF6-P flow meters and are manually balanced at around 27-28 cm<sup>3</sup> min<sup>-1</sup> before every analysis by  
adjusting the crimping of ~~the~~ both 316 stainless steel capillaries. Sample and standard gas streams ~~each flow~~ are both dried  
195 before entering the pressure stabilization chamber (C in Fig. 2) by flowing through a -80°C cold U-shaped cold traps made  
from about 25 cm of 1/4" stainless steel tubing. ~~The traps are held at about -80°C by submerging the metal tubing in a dry ice~~  
~~and ethanol mixture for the duration of the analysis before entering the pressure stabilization chamber (Fig. 2D).~~

## 2.5 Converting $\delta(\text{He}/\text{M})$ to $\delta(\text{He}/\text{N}_2)$

$\delta(\text{He}/\text{M})$  can be related to  $\delta(\text{He}/\text{N}_2)$  using

$$\delta(\text{He}/\text{N}_2) \simeq \delta(\text{He}/\text{M}) + \delta(\text{O}_2/\text{N}_2)X_{\text{O}_2} + \delta(\text{Ar}/\text{N}_2)X_{\text{Ar}} + dX_{\text{CO}_2} \quad (3)$$

200 as derived in Box 1, using independent measurements of  $\delta(\text{O}_2/\text{N}_2)$ ,  $\delta(\text{Ar}/\text{N}_2)$ , and  $dX_{\text{CO}_2}$  (Keeling et al., 2004, 1998). These  
corrections are relatively small and therefore do not significantly contribute to the overall uncertainty of  $\delta(\text{He}/\text{N}_2)$ . Analytical  
uncertainty for measurements of  $\delta(\text{O}_2/\text{N}_2)$ ,  $\delta(\text{Ar}/\text{N}_2)$ , and  $dX_{\text{CO}_2}$  is typically better than 1.5 per meg, 11 per meg, and 0.2 ppm  
(Keeling et al., 1998, 2004), yielding uncertainties of 0.3, 0.11 and 0.2 per meg in the terms  $\delta\left(\frac{\text{O}_2}{\text{N}_2}\right)X_{\text{O}_2}$ ,  $\delta(\text{Ar}/\text{N}_2)X_{\text{Ar}}$ , and  
 $dX_{\text{CO}_2}$ . The long-term atmospheric changes in  $\delta(\text{O}_2/\text{N}_2) \sim -19$  per meg yr<sup>-1</sup> and  $dX_{\text{CO}_2} \sim 2.5$  ppm yr<sup>-1</sup> yield corrections of  
205 approximately -4 per meg yr<sup>-1</sup> and +2.5 per meg yr<sup>-1</sup>, respectively. The seasonal variations in  $\delta(\text{O}_2/\text{N}_2)X_{\text{O}_2}$  and  $dX_{\text{CO}_2}$  partly  
cancel, yielding net seasonal corrections of  $\sim 10$  per meg in both hemispheres. The term  $\delta(\text{Ar}/\text{N}_2)X_{\text{Ar}}$  contributes variations less  
than 1 per meg on all time scales.

### Box 1. Deriving the helium-to-nitrogen ratio from $\delta(\text{He}/\text{M})$

A relationship between  $\delta(\text{He}/\text{N}_2)$  and  $\delta(\text{He}/\text{M})$  can be derived from:

$$\delta(\text{He}/\text{N}_2) = \frac{d\text{He}}{\text{He}} - \frac{d\text{N}_2}{\text{N}_2} = \frac{d\text{He}}{\text{He}} - \frac{d\text{M}}{\text{M}} - \frac{d\text{N}_2}{\text{N}_2} + \frac{d\text{M}}{\text{M}} = \delta(\text{He}/\text{M}) - \frac{d\text{N}_2}{\text{N}_2} + \frac{d\text{N}_2 + d\text{O}_2 + d\text{Ar} + d\text{CO}_2}{\text{M}}$$

Using  $\frac{d\text{N}_2}{\text{M}} = \frac{d\text{N}_2}{\text{N}_2} X_{\text{N}_2}$ ,  $\frac{d\text{O}_2}{\text{M}} = \frac{d\text{O}_2}{\text{O}_2} X_{\text{O}_2}$ , etc, where  $X_i$  is the mole fraction of gas  $i$ , yields

$$\begin{aligned} \delta(\text{He}/\text{N}_2) = \delta(\text{He}/\text{M}) + \frac{d\text{N}_2}{\text{N}_2} [-1 + X_{\text{N}_2} + X_{\text{O}_2} + X_{\text{Ar}} + X_{\text{CO}_2} + X_{\text{H}_2\text{O}} \dots] + \left[ \frac{d\text{O}_2}{\text{O}_2} - \frac{d\text{N}_2}{\text{N}_2} \right] X_{\text{O}_2} + \left[ \frac{d\text{Ar}}{\text{Ar}} - \frac{d\text{N}_2}{\text{N}_2} \right] X_{\text{Ar}} \\ + \left[ \frac{d\text{CO}_2}{\text{CO}_2} - \frac{d\text{N}_2}{\text{N}_2} \right] X_{\text{CO}_2} + \dots \end{aligned}$$

This can be simplified to Eq. (3) using  $\left[ \frac{d\text{CO}_2}{\text{CO}_2} - \frac{d\text{N}_2}{\text{N}_2} \right] X_{\text{CO}_2} = dX_{\text{CO}_2}$ , which follows because relative changes in  $\text{CO}_2$  are much larger than relative changes in  $\text{N}_2$ .

## 3 Results

### 210 3.1 Gettering performance

A mass scan of ~~medical~~ air introduced through the gettering and flow-stabilizing inlet system revealed that  $\text{N}_2$  and  $\text{O}_2$  are almost completely removed from the air by the on-line getter (Fig. 4). He is effectively preconcentrated in the gas mixture.  $^{40}\text{Ar}$  ions with one or more charges yield the largest beams in the scan followed by  $^{36}\text{Ar}$ , and  $\text{H}_2$  evolving from the hot metal in the getter oven.

### 215 3.2 Response time

Our setup demonstrates the ability to transition between sample and standard gas with a e-folding time scale of  $\sim 4$  seconds (Fig. 5). The e-folding time is primarily controlled by the volume of the getter and the total flow of gas through the getter. Regions of the inlet system upstream of the getter experience  $\sim 100\times$  faster flushing than downstream of the getter because the gas upstream still contains  $\text{N}_2$  and  $\text{O}_2$  and hence flows much faster. An associated large drop in pressure however ensures that  
220 all parts of the inlet system are flushed out similarly quickly. The e-folding time does not change substantially over the life span of the getter.

### 3.3 Analytical precision

Using the default 60 sec sample-standard cycle, the gettering and flow-stabilizing inlet system achieves an internal precision in  $\delta(\text{He}/\text{M})$  of approximately  $\pm 15$  per meg over 1.5h and  $\pm 8$  per meg ( ~~$\pm 6$~~ ) for samples run 6h or longer ( $1\sigma$ , standard error of  
225  $\sim 90$  and  $\sim 360$  cycles respectively) (Figs. 6&7). The (external) reproducibility of repeated 6–8h measurements of the same

sample and standard gas cylinder combination is comparable and essentially as expected from the shot-noise on the  $^4\text{He}$  ion current (Figs. 6&7).

The zero enrichment, i.e., the delta value observed when introducing the same gas through sample and standard side of the inlet, is generally small and stable over time. It is tested by mounting the crimped delivery capillaries (A in Fig. 2A) to a tee fitting, which splits the gas stream at high pressure from a single tank of air. This tee minimizes thermal fractionation by dividing the flow at a junction machined into the center of a large brass block (Keeling, 1988). Identical delta values (within error) obtained after reversing the outlet from the tee demonstrate that no measurable fractionation occurs within the tee and therefore that the zero enrichment reflects a persistent asymmetry somewhere downstream, most likely within the ~~open split~~ pressure stabilization chamber. The typical zero enrichment varies slightly with the mean flow of gas into the stabilization chamber (F), the pressure in the chamber (P), and the flow offset between SA and ST side ( $\Delta F$ ) before entering the stabilization chamber (Fig. 7). Weighted multiple linear regression analysis using 3 different pressure levels (9 psi, 14 psi, and 16 psi, i.e., 62.1, 96.5, and 110.3 kPa) and predictors F, P, and  $\Delta F$  reveals that the zero enrichment value decreases by  $2.8 \pm 0.9$  per meg per  $1 \text{ cm}^3 \text{ min}^{-1}$  change in mean flow away from  $27.5 \text{ cm}^3 \text{ min}^{-1}$  and increases by  $17.2 \pm 4.8$  per meg per  $1 \text{ cm}^3 \text{ min}^{-1}$  flow imbalance between SA and ST ( $1\sigma$ ). The analysis also finds that the dependence of  $\delta(\text{He}/M)$  on F and  $\Delta F$  is significant at the 5% level. For a balanced flow of  $27.5 \text{ cm}^3 \text{ min}^{-1}$  ~~at and a pressure of 62.19, 96.514 and 110.3 kPa 16 psi pressure~~ in the stabilization chamber, the mean zero enrichment is  $-9.61 \pm 7.2$  ~~per meg~~,  $1 \pm 3.7$  ~~per meg~~ and  $-15.7 \pm 4.7$  per meg, respectively. For actual measurements, P is held constant ~~for measurements at 96.514 psikPa with very high precision~~. F and  $\Delta F$  are stable over 8h to within  $\pm 0.2 \text{ cm}^3 \text{ min}^{-1}$ . This typically yields a correction for mean gas flow and flow imbalance of less than 10 per meg with an uncertainty smaller than 6 per meg, which increases the overall analytical uncertainty in repeat tank analysis from 8 to 10 per meg.

#### 4 Discussion

The gettering and flow-stabilizing inlet system has demonstrated the ability to determine the helium mole fraction difference between a sample and standard gas,  $\delta(\text{He}/M)$ , to about 10 per meg in a single 6–8h analysis and has a range of possible applications.  ~~$\delta(\text{He}/M)$  can be related to  $\delta(\text{He}/N_2)$  using~~

$$\delta(\text{He}/N_2) \approx \delta(\text{He}/M) + \delta(\text{O}_2/N_2)X_{\text{O}_2} + \delta(\text{Ar}/N_2)X_{\text{Ar}} + dX_{\text{CO}_2} \quad (1)$$

~~as derived in Box 1, using independent measurements of  $\delta(\text{O}_2/N_2)$ ,  $\delta(\text{Ar}/N_2)$ , and  $dX_{\text{CO}_2}$  (Keeling et al., 2004, 1998). These corrections are relatively small and therefore do not significantly contribute to the overall uncertainty of  $\delta(\text{He}/N_2)$ . The long-term atmospheric changes in  $\delta(\text{O}_2/N_2)$   $-19$  per meg  $\text{yr}^{-1}$  and  $dX_{\text{CO}_2}$   $-2.5$  ppm  $\text{yr}^{-1}$  yield corrections of approximately  $-4$  per meg  $\text{yr}^{-1}$  and  $+2.5$  per meg  $\text{yr}^{-1}$ , respectively. The seasonal variations in  $\delta(\text{O}_2/N_2)X_{\text{O}_2}$  and  $dX_{\text{CO}_2}$  partly cancel, yielding net seasonal corrections of  $-10$  per meg in both hemispheres. The term  $\delta(\text{Ar}/N_2)X_{\text{Ar}}$  contributes variations less than 1 per meg on all time scales.~~

### Box 1. Deriving the helium-to-nitrogen ratio from $\delta(\text{He}/M)$

A relationship between  $\delta(\text{He}/N_2)$  and  $\delta(\text{He}/M)$  can be derived from:

$$\delta(\text{He}/N_2) = \frac{d\text{He}}{\text{He}} \frac{dN_2}{N_2} = \frac{d\text{He}}{\text{He}} \frac{dM}{M} \frac{dN_2}{N_2} + \frac{dM}{M} = \delta(\text{He}/M) \frac{dN_2}{N_2} + \frac{dN_2 + dO_2 + dAr + dCO_2}{M}$$

Using  $\frac{dN_x}{M} = \frac{dN_x}{N_x} X_{N_x}$ ,  $\frac{dO_2}{M} = \frac{dO_2}{O_2} X_{O_2}$ , etc, where  $X_i$  is the mole fraction of gas  $i$ , yields

$$\delta(\text{He}/N_2) = \delta(\text{He}/M) + \frac{dN_2}{N_2} [1 + X_{N_2} + X_{O_2} + X_{Ar} + X_{CO_2} + X_{H_2O} \dots] + \left[ \frac{dO_2}{O_2} \frac{dN_2}{N_2} \right] X_{O_2} + \left[ \frac{dAr}{Ar} \frac{dN_2}{N_2} \right] X_{Ar} \\ + \left[ \frac{dCO_2}{CO_2} \frac{dN_2}{N_2} \right] X_{CO_2} + \dots$$

This can be simplified to Eq. (3) using  $\left[ \frac{dCO_2}{CO_2} \frac{dN_2}{N_2} \right] X_{CO_2} = dX_{CO_2}$ , which follows because relative changes in  $CO_2$  are much larger than relative changes in  $N_2$ .

#### 4.1 — Potential applications

~~The presented He/N<sub>2</sub> measurement capability has a range of possible applications.~~ Our primary targets are (i) to use stratospheric  $\delta(\text{He}/N_2)$  as a tracer of the large-scale stratospheric circulation and (ii) to evaluate tropospheric  $\delta(\text{He}/N_2)$  trends as a possible indicator of anthropogenic fossil fuel exploitation.

We expect an excellent signal-to-noise ratio for the detection of stratospheric changes in  $\delta(\text{He}/N_2)$ . Interannual variability in stratospheric  $\delta(\text{He}/N_2)$  is likely on the order 300–400 per meg (Table 1). Repeat 6–8h measurements of a high-pressure ~~tank cylinder~~ currently achieve a precision of ~10 per meg, or about 40 times better than the stratospheric signal. Associated changes in tropospheric  $\delta(\text{He}/N_2)$ , in contrast, are likely much smaller at around 6 per meg and therefore at or below the current limit of detection even after averaging of multiple samples.

~~The reproducibility of measurements also depends on adequate calibration strategies. The short term reproducibility of high-pressure cylinders shown in Figure 6 and the long term stability established for O<sub>2</sub>/N<sub>2</sub>, CO<sub>2</sub>, and Ar/N<sub>2</sub> standard gases in previous work (Keeling et al., 2007) suggest long term stability in  $\delta(\text{He}/N_2)$  is achievable but needs further evaluation.~~

He/N<sub>2</sub> measurements can help quantify the anthropogenic <sup>4</sup>He release over time due to fossil fuel extraction (Boucher et al., 2018c; Lupton and Evans, 2013, 2004; Mabry et al., 2015; Oliver et al., 1984; Sano et al., 2010, 1989). Although theoretical predictions clearly support an anthropogenic <sup>4</sup>He increase, past observational studies produced conflicting evidence. Recent improvements in analytical methods and sampling have narrowed the uncertainty in <sup>3</sup>He/<sup>4</sup>He trend estimates to <30 per meg y<sup>-1</sup> with a mean statistically indistinguishable from zero (Table 1). However, with a precision of ~10 per meg on single samples, measurements of  $\delta(^4\text{He}/N_2)$  on decades-old archived air may allow trend detection to ~1 per meg y<sup>-1</sup> or better, while also avoiding possible complications from <sup>3</sup>He emissions that could bias estimates of the <sup>4</sup>He source from <sup>3</sup>He/<sup>4</sup>He.

Another possible application is the investigation of spatial gradients in atmospheric  $\delta(\text{He}/\text{N}_2)$  caused by the distribution of local volcanic or anthropogenic sources (e.g., Sano et al., 2010; Boucher et al., 2018c). High precision  $\delta(\text{He}/\text{N}_2)$  may allow the detection of diffuse helium release in regions of volcanic activity (Boucher et al., 2018b). Furthermore, global north-south  $\delta(\text{He}/\text{N}_2)$  gradients from anthropogenic emission sources concentrated in the Northern Hemisphere are likely on the order of  
280 10s of per meg and thus may also be detectable directly. Alternatively, studies could target more local gradients around oil or natural gas facilities that are likely even greater.

The method developed here is potentially applicable to measure the abundance of any noble gas in air. The intensity of the ion beam and thus the precision for different noble gases depends on their natural abundance and ionization efficiency in the MS source.  $^{20}\text{Ne}$  and  $^{22}\text{Ne}$  have isobaric interferences from doubly charged Ar and  $\text{CO}_2$ , but Kr and Xe yield usable ion beams  
285 (Table 2). We estimate a precision of  $\sim 5$  and  $\sim 19$  per meg for repeat 6–8h analyses of  $\delta(^{84}\text{Kr}/^{28}\text{N}_2)$  and  $\delta(^{132}\text{Xe}/^{28}\text{N}_2)$  respectively, by assuming that precision scales with the square root of the total ions counted as expected from shot-noise behavior. This estimate compares favorably to the precision currently reported in conventional dual inlet mass spectrometry studies (Baggenstos et al., 2019; Bereiter et al., 2018). For example, Baggenstos et al. (2019) achieved a precision of 88 per meg and 203 per meg for repeat  $\sim 2$ h analyses of  $\delta(^{84}\text{Kr}/^{40}\text{Ar})$  and  $\delta(^{132}\text{Xe}/^{40}\text{Ar})$  in ambient air, respectively.

The improved precision enabled by our inlet system should be sufficient to resolve the previously unobserved annual cycle of Kr and Xe caused by the seasonal release and uptake of both gases by the ocean as it warms and cools. The seasonal cycle of  $\delta(^{40}\text{Ar}/^{28}\text{N}_2)$  has an amplitude of 5–15 per meg in the extratropics (Keeling et al., 2004).  $\delta(^{84}\text{Kr}/^{28}\text{N}_2)$  and  $\delta(^{132}\text{Xe}/^{28}\text{N}_2)$  however are  $\sim 3.4$  and  $\sim 8.9$  times more sensitive than  $\delta(^{40}\text{Ar}/^{28}\text{N}_2)$  to changes in ocean temperature owing to the different temperature-dependences of Ar, Kr and Xe solubility in seawater (Hamme and Emerson, 2004; Jenkins et al., 2019). This implies that  
290 seasonal variations in  $\delta(^{84}\text{Kr}/^{28}\text{N}_2)$  and  $\delta(^{132}\text{Xe}/^{28}\text{N}_2)$  have a magnitude of 17–51 and 45–134 per meg respectively, which would be readily resolved if precision of our system scales as expected with signal strength.

The gettering inlet and MS system was applied here only for single ion ( $\text{He}^+$ ) detection, but alternately could be applied for multi-ion collection. The acquisition of Kr and Xe isotope ratios for example would provide valuable additional information for detecting artefactual fractionation during sampling and allow further improvements in precision by increasing the total  
300 number of ions collected.

The need for only a single ion detector also allows the gettering and flow-stabilizing inlet to be interfaced with simpler and more affordable mass spectrometers, such as quadrupole systems. The performance of the system will depend on the stability of the  $^4\text{He}^+$ -ion beam over the time scale of switching and will need to be evaluated critically, but any variability on time scales longer than the switching time is canceled by sample-standard differencing.

305 Additional work is needed to further improve calibration methods and to establish standard procedures for collecting air samples while avoiding artifacts in  $\text{He}/\text{N}_2$  at the 10 per meg level. We currently need samples of  $\sim 16$ -20l for a full 8h analysis because long purging and analysis times are necessary to achieve a precision of 10 per meg. If reduced precision is acceptable, analyses time can be shortened but purging of the inlet system for at least one hour is needed before each analysis even for lower precision work. Furthermore, air samples must currently be provided at pressure greater than 3 atm to allow sufficient

310 flow through the narrow tubing into the pressure-stabilization chamber. The reproducibility of measurements also depends on adequate calibration strategies. The short-term reproducibility of high-pressure cylinders shown in Figure 6 and the long-term stability established for O<sub>2</sub>/N<sub>2</sub>, CO<sub>2</sub>, and Ar/N<sub>2</sub> standard gases in previous work (Keeling et al., 2007) suggest that long-term stability in  $\delta(\text{He}/\text{N}_2)$  is achievable but needs further evaluation.

## 5 Conclusions

315 Here, we presented a new method for high-precision measurements of changes in the <sup>4</sup>He mole fraction He/N<sub>2</sub> ratio of atmospheric air which can be directly related to changes in He/N<sub>2</sub> ratio. The method relies on monitoring of the <sup>4</sup>He<sup>+</sup> ion beam in a mass spectrometer during sample-standard switching. The ion beam is stabilized by flowing sample and standard air through a single capillary into the MS from an actively pressure-controlled open-split (Henneberg et al., 1975), such that variability of the <sup>4</sup>He<sup>+</sup> ion beam directly reflects differences in the helium mole fraction of the gas mixtures. Measurements of  
320 the helium mole fraction can easily be converted to  $\delta(\text{He}/\text{N}_2)$  ~~after the analysis~~ if O<sub>2</sub>/N<sub>2</sub>, Ar/N<sub>2</sub>, and CO<sub>2</sub> concentrations of the sample are determined as well. An online getter preconcentrates He and other noble gases before entry into the MS by chemically removing >99.99-% of all N<sub>2</sub> and O<sub>2</sub> in a reaction with titanium sponge. Our method thereby avoids the need for peak jumping and ~~avoids the need for~~ a multi-collector mass spectrometer, while achieving a precision of ~10 per meg (1 $\sigma$ ) on repeat analysis of  $\delta(\text{He}/\text{N}_2)$  in high-pressure tanks.

325 In future work, the gettering and flow-stabilizing inlet system could be used to investigate possible interannual to decadal changes in stratospheric  $\delta(\text{He}/\text{N}_2)$  linked to variability in stratospheric circulation and stratosphere-troposphere exchange processes. Additional applications could include the search for a signal of anthropogenic helium release during fossil fuel extraction and burning (~~Boucher et al., 2018c; Lupton and Evans, 2013, 2004; Mabry et al., 2015; Oliver et al., 1984; Pierson-Wickmann et al., 2001; Sano et al., 1989~~), or measurements of spatial gradients resulting from localized human or natural  
330 sources of helium (~~Boucher et al., 2018a, 2018b; Sano et al., 2010~~). The setup is also suitable for the analysis of other noble gases and could therefore be used to study seasonal ocean warming associated with degassing or uptake of Kr and Xe from the ocean (Baggenstos et al., 2019; Bereiter et al., 2018).

## 6 Acknowledgements

We thank Ross Beaudette, Alan Seltzer, Sarah Shackleton, Jacob Morgen, Jessica Ng, and Eric Morgan for laboratory support  
335 and insightful discussions during the development of the He/N<sub>2</sub> analysis system. We are grateful to Shane Clark, Savannah Hatley, Adam Cox, and Timothy Lueker for providing high-pressure cylinders used during testing. We also thank them for maintaining and operating the Ar/N<sub>2</sub>, O<sub>2</sub>/N<sub>2</sub> and CO<sub>2</sub> analysis systems in the Keeling laboratory. This work was supported by the National Science Foundation grants MRI-1920369 and AGS-1940361.

## 7 Data availability

340 Data presented in this manuscript are available as an electronic supplement to this paper from the journal website.

## 8 Competing interests

The authors declare that they have no conflict of interest.

## 9 Author contribution

BB designed and build the inlet system with important design expertise from WP, JS and RK. BB performed all testing and  
345 prepared the manuscript with contributions from all co-authors.

## 10 References

- Arblaster, J.M., Gillett, N.P., Calvo, N., Forster, P.M., Polvani, L.M., Son, S.-W., Waugh, D.W., Young, P.J., 2014. Stratospheric ozone changes and climate, Chapter 4, Scientific Assessment of Ozone Depletion: 2014, Global Ozone Research and Monitoring Project – Report No. 55. Geneva, Switzerland.
- 350 Baggenstos, D., Häberli, M., Schmitt, J., Shackleton, S.A., Birner, B., Severinghaus, J.P., Kellerhals, T., Fischer, H., 2019. Earth's radiative imbalance from the Last Glacial Maximum to the present. *Proc. Natl. Acad. Sci. U. S. A.* 116, 14881–14886. <https://doi.org/10.1073/pnas.1905447116>
- Belikov, D., Sugawara, S., Ishidoya, S., Hasebe, F., Maksyutov, S., Aoki, S., Morimoto, S., Nakazawa, T., 2019. Three-dimensional simulation of stratospheric gravitational separation using the NIES global atmospheric tracer transport  
355 model. *Atmos. Chem. Phys.* 19, 5349–5361. <https://doi.org/10.5194/acp-19-5349-2019>
- Bereiter, B., Shackleton, S., Baggenstos, D., Kawamura, K., Severinghaus, J., 2018. Mean global ocean temperatures during the last glacial transition. *Nature* 553, 39–44. <https://doi.org/10.1038/nature25152>
- Birner, B., Chipperfield, M.P., Morgan, E.J., Stephens, B.B., Linz, M., Feng, W., Wilson, C., Bent, J.D., Wofsy, S.C., Severinghaus, J., Keeling, R.F., 2020. Gravitational separation of Ar/N<sub>2</sub> and age of air in the lowermost stratosphere in  
360 airborne observations and a chemical transport model. *Atmos. Chem. Phys. Discuss.* 1–34. <https://doi.org/10.5194/acp-2020-95>
- Bönisch, H., Engel, A., Curtius, J., Birner, T., Hoor, P., 2009. Quantifying transport into the lowermost stratosphere using simultaneous in-situ measurements of SF<sub>6</sub> and CO<sub>2</sub>. *Atmos. Chem. Phys.* 9, 5905–5919. <https://doi.org/10.5194/acp-9-5905-2009>
- 365 Boucher, C., Lan, T., Mabry, J., Bekaert, D. V., Burnard, P.G., Marty, B., 2018a. Spatial analysis of the atmospheric helium isotopic composition: Geochemical and environmental implications. *Geochim. Cosmochim. Acta* 237, 120–130.

<https://doi.org/10.1016/j.gca.2018.06.010>

- Boucher, C., Lan, T., Marty, B., Burnard, P.G., Fischer, T.P., Ayalew, D., Mabry, J., Maarten de Moor, J., Zelenski, M.E., Zimmermann, L., 2018b. Atmospheric helium isotope composition as a tracer of volcanic emissions: A case study of  
370 Erta Ale volcano, Ethiopia. *Chem. Geol.* 480, 3–11. <https://doi.org/10.1016/j.chemgeo.2017.05.011>
- Boucher, C., Marty, B., Zimmermann, L., Langenfelds, R., 2018c. Atmospheric helium isotopic ratio from 1910 to 2016 recorded in stainless steel containers. *Geochemical Perspect. Lett.* 6, 23–27. <https://doi.org/10.7185/geochemlet.1804>
- Brewer, A.W., 1949. Evidence for a world circulation provided by the measurements of helium and water vapour distribution in the stratosphere. *Q. J. R. Meteorol. Soc.* 75, 351–363. <https://doi.org/10.1002/qj.49707532603>
- 375 Butchart, N., 2014. The Brewer-Dobson circulation. *Rev. Geophys.* 52, 157–184. <https://doi.org/10.1002/2013RG000448>
- Dobson, G.M.B., 1956. Origin and distribution of the polyatomic molecules in the atmosphere. *Proc. R. Soc. London. Ser. A. Math. Phys. Sci.* 236, 187–193. <https://doi.org/10.1098/rspa.1956.0127>
- Engel, A., Bönisch, H., Ullrich, M., Sitals, R., Membrive, O., Danis, F., Crevoisier, C., 2017. Mean age of stratospheric air derived from AirCore observations. *Atmos. Chem. Phys.* 17, 6825–6838. <https://doi.org/10.5194/acp-17-6825-2017>
- 380 Engel, A., Möbius, T., Bönisch, H., Schmidt, U., Heinz, R., Levin, I., Atlas, E., Aoki, S., Nakazawa, T., Sugawara, S., Moore, F., Hurst, D., Elkins, J., Schauffler, S., Andrews, A., Boering, K., 2009. Age of stratospheric air unchanged within uncertainties over the past 30 years. *Nat. Geosci.* 2, 28–31. <https://doi.org/10.1038/ngeo388>
- Flury, T., Wu, D.L., Read, W.G., 2013. Variability in the speed of the Brewer-Dobson circulation as observed by Aura/MLS. *Atmos. Chem. Phys.* 13, 4563–4575. <https://doi.org/10.5194/acp-13-4563-2013>
- 385 Fowler, D., Coyle, M., Skiba, U., Sutton, M.A., Cape, J.N., Reis, S., Sheppard, L.J., Jenkins, A., Grizzetti, B., Galloway, J.N., Vitousek, P., Leach, A., Bouwman, A.F., Butterbach-Bahl, K., Dentener, F., Stevenson, D., Amann, M., Voss, M., 2013. The global nitrogen cycle in the Twentyfirst century. *Philos. Trans. R. Soc. B Biol. Sci.* 368. <https://doi.org/10.1098/rstb.2013.0164>
- Glückauf, E., 1944. A simple analysis of the helium content of air. *Trans. Faraday Soc.* 44, 436–439.
- 390 Graven, H.D., Guilderson, T.P., Keeling, R.F., 2012. Observations of radiocarbon in CO<sub>2</sub> at La Jolla, California, USA 1992–2007: Analysis of the long-term trend. *J. Geophys. Res. Atmos.* 117, 1–14. <https://doi.org/10.1029/2011JD016533>
- Haenel, F.J., Stiller, G.P., Von Clarmann, T., Funke, B., Eckert, E., Glatthor, N., Grabowski, U., Kellmann, S., Kiefer, M., Linden, A., Reddmann, T., 2015. Reassessment of MIPAS age of air trends and variability. *Atmos. Chem. Phys.* 15, 13161–13176. <https://doi.org/10.5194/acp-15-13161-2015>
- 395 Hamilton, K., Fan, S.-M., 2000. Effects of the stratospheric quasi-biennial oscillation on long-lived greenhouse gases in the troposphere. *J. Geophys. Res.* 105, 20581. <https://doi.org/10.1029/2000JD900331>
- Hamme, R.C., Emerson, S.R., 2004. The solubility of neon, nitrogen and argon in distilled water and seawater. *Deep. Res. I* 51, 1517–1528.
- Hegglin, M.I., Shepherd, T.G., 2009. Large climate-induced changes in ultraviolet index and stratosphere-to-troposphere  
400 ozone flux. *Nat. Geosci.* 2, 687–691. <https://doi.org/10.1038/ngeo604>

- Henneberg, D., Heinrichs, U., Schomburg, G., 1975. Open Split Connection of Glass Capillary Columns to Mass Spectrometers. *Chromatographia* 8, 449–451.
- Holland, P.W., Emerson, D.E., 1987. A determination of the helium 4 content of near-surface atmospheric air within the continental United States. *J. Geophys. Res. Solid Earth* 92, 12557–12566.
- 405 Holton, J.R., Haynes, P.H., McIntyre, M.E., Douglass, A.R., Rood, B., 1995. Stratosphere-Troposphere. *Rev. Geophys.* 403–439.
- Ishidoya, S., Sugawara, S., Inai, Y., Morimoto, S., Honda, H., Ikeda, C., Hashida, G., Machida, T., Tomikawa, Y., Toyoda, S., Goto, D., Aoki, S., Nakazawa, T., 2018. Gravitational separation of the stratospheric air over Syowa, Antarctica and its connection with meteorological fields. *Atmos. Sci. Lett.* 19, 1–7. <https://doi.org/10.1002/asl.857>
- 410 Ishidoya, S., Sugawara, S., Morimoto, S., Aoki, S., Nakazawa, T., 2008. Gravitational separation of major atmospheric components of nitrogen and oxygen in the stratosphere. *Geophys. Res. Lett.* 35. <https://doi.org/10.1029/2007GL030456>
- Ishidoya, S., Sugawara, S., Morimoto, S., Aoki, S., Nakazawa, T., Honda, H., Murayama, S., 2013. Gravitational separation in the stratosphere - A new indicator of atmospheric circulation. *Atmos. Chem. Phys.* 13, 8787–8796. <https://doi.org/10.5194/acp-13-8787-2013>
- 415 Ishidoya, S., Sugawara, S., Tohjima, Y., Goto, D., Ishijima, K., Niwa, Y., Aoki, N., Murayama, S., 2020. Secular change of the atmospheric Ar/N<sub>2</sub> and its implications for ocean heat uptake and Brewer-Dobson circulation. *Atmos. Chem. Phys. Discuss.* <https://doi.org/doi.org/10.5194/acp-2020-301>
- Jenkins, W.J., Lott, D.E., Cahill, K.L., 2019. A determination of atmospheric helium, neon, argon, krypton, and xenon solubility concentrations in water and seawater. *Mar. Chem.* 211, 94–107. <https://doi.org/10.1016/j.marchem.2019.03.007>
- 420 Keeling, R.F., 1988. Development of an interferometric oxygen analyzer for precise measurement of the atmospheric O<sub>2</sub> mole fraction. Harvard University.
- Keeling, R.F., Blaine, T., Paplawsky, B., Katz, L., Atwood, C., Brockwell, T., 2004. Measurement of changes in atmospheric Ar/N<sub>2</sub> ratio using a rapid-switching, single-capillary mass spectrometer system. *Tellus* 56B, 322–338. <https://doi.org/10.1111/j.1600-0889.2004.00117.x>
- 425 Keeling, R.F., Manning, A.C., McEvoy, E.M., Shertz, S.R., 1998. Methods for measuring changes in atmospheric O<sub>2</sub> concentration and their application in southern hemisphere air. *J. Geophys. Res.* 103, 3381–3397. <https://doi.org/10.1029/97JD02537>
- Keeling, R.F., Manning, A.C., Paplawsky, W.J., Cox, A.C., 2007. On the long-term stability of reference gases for atmospheric O<sub>2</sub>/N<sub>2</sub> and CO<sub>2</sub> measurements. *Tellus B Chem. Phys. Meteorol.* 59B, 3–14. <https://doi.org/10.1111/j.1600-0889.2006.00196.x>
- 430 Kockarts, G., 1973. Helium in the terrestrial atmosphere. *Space Sci. Rev.* 14, 723–757. <https://doi.org/10.1007/BF00224775>
- Li, F., Waugh, D.W., Douglass, A.R., Newman, P.A., Pawson, S., Stolarski, R.S., Strahan, S.E., Nielsen, J.E., 2012. Seasonal variations of stratospheric age spectra in the Goddard Earth Observing System Chemistry Climate Model (GEOSCCM).

- 435 J. Geophys. Res. Atmos. 117, 1–14. <https://doi.org/10.1029/2011JD016877>
- Lupton, J., Evans, L., 2013. Changes in the atmospheric helium isotope ratio over the past 40 years. *Geophys. Res. Lett.* 40, 6271–6275. <https://doi.org/10.1002/2013GL057681>
- Lupton, J., Evans, L., 2004. The atmospheric helium isotope ratio: Is it changing? *Geophys. Res. Lett.* 31, 1–4. <https://doi.org/10.1029/2004GL020041>
- 440 Mabry, J.C., Lan, T., Boucher, C., Burnard, P.G., Brennwald, M.S., Langenfelds, R., Marty, B., 2015. No evidence for change of the atmospheric helium isotope composition since 1978 from re-analysis of the Cape Grim Air Archive. *Earth Planet. Sci. Lett.* 428, 134–138. <https://doi.org/10.1016/j.epsl.2015.07.035>
- Montzka, S.A., Dutton, G.S., Yu, P., Ray, E., Portmann, R.W., Daniel, J.S., Kuijpers, L., Hall, B.D., Mondeel, D., Siso, C., Nance, J.D., Rigby, M., Manning, A.J., Hu, L., Moore, F., Miller, B.R., Elkins, J.W., 2018. An unexpected and persistent  
445 increase in global emissions of ozone-depleting CFC-11. *Nature* 557, 413–417. <https://doi.org/10.1038/s41586-018-0106-2>
- Nevison, C.D., Dlugokencky, E., Dutton, G., Elkins, J.W., Fraser, P., Hall, B., Krummel, P.B., Langenfelds, R.L., O’Doherty, S., Prinn, R.G., Steele, L.P., Weiss, R.F., 2011. Exploring causes of interannual variability in the seasonal cycles of tropospheric nitrous oxide. *Atmos. Chem. Phys.* 11, 3713–3730. <https://doi.org/10.5194/acp-11-3713-2011>
- 450 Oliver, B.M., Bradley, J.G., Farrar IV, H., 1984. Helium concentration in the Earth’s lower atmosphere. *Geochim. Cosmochim. Acta* 48, 1759–1767. [https://doi.org/10.1016/0016-7037\(84\)90030-9](https://doi.org/10.1016/0016-7037(84)90030-9)
- Pierson-Wickmann, A.C., Marty, B., Ploquin, A., 2001. Helium trapped in historical slags: A search for temporal variation of the He isotopic composition of air. *Earth Planet. Sci. Lett.* 194, 165–175. [https://doi.org/10.1016/S0012-821X\(01\)00554-4](https://doi.org/10.1016/S0012-821X(01)00554-4)
- 455 Ray, E.A., Moore, F.L., Rosenlof, K.H., Davis, S.M., Boenisch, H., Morgenstern, O., Smale, D., Rozanov, E., Hegglin, M., Pitari, G., Mancini, E., Braesicke, P., Butchart, N., Hardiman, S., Li, F., Shibata, K., Plummer, D.A., 2010. Evidence for changes in stratospheric transport and mixing over the past three decades based on multiple data sets and tropical leaky pipe analysis. *J. Geophys. Res. Atmos.* 115, 1–16. <https://doi.org/10.1029/2010JD014206>
- Ray, E.A., Moore, F.L., Rosenlof, K.H., Davis, S.M., Sweeney, C., Tans, P., Wang, T., Elkins, J.W., Bönisch, H., Engel, A.,  
460 Sugawara, S., Nakazawa, T., Aoki, S., 2014. Improving stratospheric transport trend analysis based on SF<sub>6</sub> and CO<sub>2</sub> measurements. *J. Geophys. Res. Atmos.* 119, 14110–14128. <https://doi.org/10.1002/2014JD021802>
- Reid, R.C., Prausnitz, J.M., Poling, B.E., 1987. *The properties of gases and liquids*, 4th ed. McGraw-Hill, New York.
- Salby, M.L., Callaghan, P.F., 2006. Influence of the Brewer-Dobson circulation on stratosphere-troposphere exchange. *J. Geophys. Res. Atmos.* 111, 1–9. <https://doi.org/10.1029/2006JD007051>
- 465 Sano, Y., Furukawa, Y., Takahata, N., 2010. Atmospheric helium isotope ratio: Possible temporal and spatial variations. *Geochim. Cosmochim. Acta* 74, 4893–4901. <https://doi.org/10.1016/j.gca.2010.06.003>
- Sano, Y., Marty, B., Burnard, P., 2013. Noble Gases in the Atmosphere, in: Burnard, P. (Ed.), *The Noble Gases as Geochemical Tracers*. Springer Berlin Heidelberg, pp. 17–31. [https://doi.org/10.1007/978-3-642-28836-4\\_2](https://doi.org/10.1007/978-3-642-28836-4_2)

- Sano, Y., Wakita, H., Makide, Y., Tominaga, T., 1989. A ten-year decrease in the atmospheric helium isotope ratio possibly caused by human activity. *Geophys. Res. Lett.* 16, 1371–1374. <https://doi.org/10.1029/GL016i012p01371>
- 470 Simmonds, P.G., Manning, A.J., Athanassiadou, M., Scaife, A.A., Derwent, R.G., O’Doherty, S., Harth, C.M., Weiss, R.F., Dutton, G.S., Hall, B.D., Sweeney, C., Elkins, J.W., 2013. Interannual fluctuations in the seasonal cycle of nitrous oxide and chlorofluorocarbons due to the Brewer-Dobson circulation. *J. Geophys. Res. Atmos.* 118, 10694–10706. <https://doi.org/10.1002/jgrd.50832>
- 475 Sugawara, S., Ishidoya, S., Aoki, S., Morimoto, S., Nakazawa, T., Toyoda, S., Inai, Y., Hasebe, F., Ikeda, C., Honda, H., Goto, D., Putri, F.A., 2018. Age and gravitational separation of the stratospheric air over Indonesia. *Atmos. Chem. Phys.* 18, 1819–1833. <https://doi.org/10.5194/acp-18-1819-2018>
- Torgersen, T., 1989. Terrestrial helium degassing fluxes and the atmospheric helium budget: Implications with respect to the degassing processes of continental crust. *Chem. Geol. Isot. Geosci. Sect.* 79, 1–14. [https://doi.org/10.1016/0168-9622\(89\)90002-X](https://doi.org/10.1016/0168-9622(89)90002-X)
- 480 Weiss, R.F., 1971. Solubility of helium and neon in water and seawater. *J. Chem. Eng. Data* 16, 235–241. <https://doi.org/10.1021/je60049a019>
- Zartman, R.E., Wasserburg, G.J., Reynolds, J.H., 1961. Helium, Argon, and Carbon in Some Natural Gases. *J. Geophys. Res.* 66, 277–306. <https://doi.org/10.1029/jz066i001p00277>

## 485 11 Figures and Figure Captions

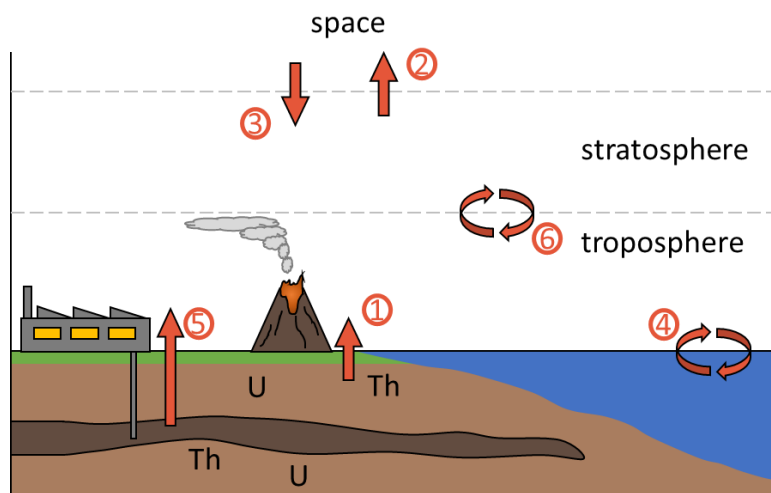
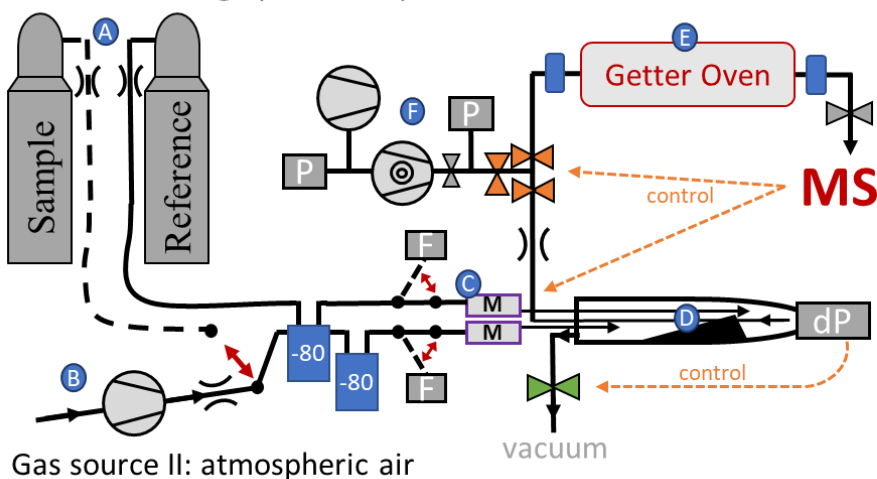


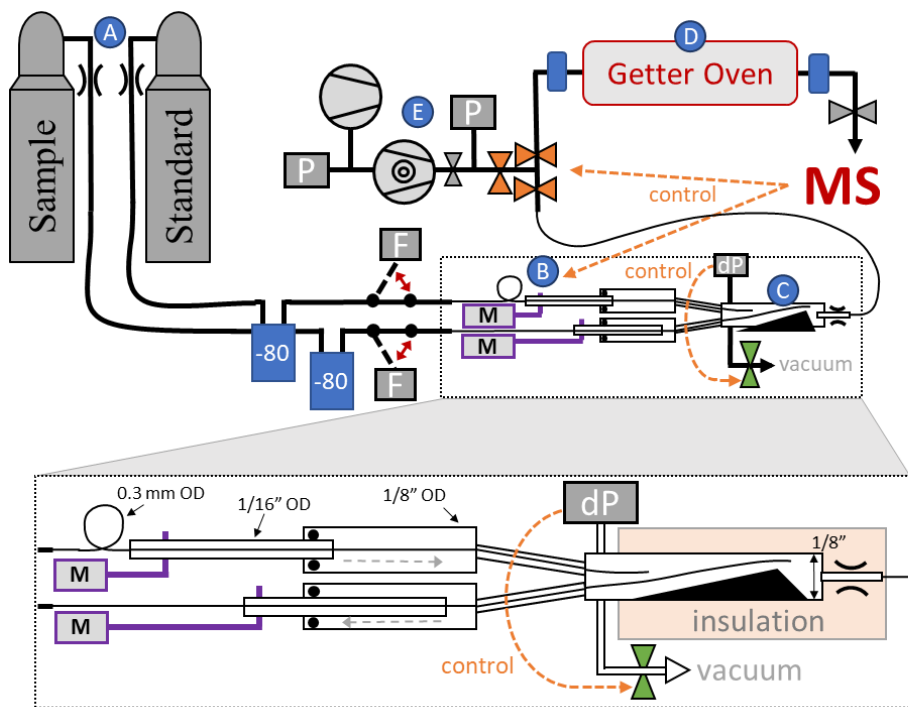
**Figure 1.** Schematic depiction of  $^4\text{He}$  fluxes to and from the troposphere. Different processes are numbered and listed in Table 1.

Gas source I: high pressure cylinders



Gas source II: atmospheric air

- ) ( capillary
- ⊗ manual shutoff valve
- P pressure gauge
- dP differential P-gauge
- F flow meter
- ⊙ pump
- ⊙ turbomolecular pump
- ⊗ change-over-valve
- M pneumatic piston
- ⊗ flow control valve
- 0.2μm filter
- 80 Dry ice water trap



- ) ( Flow restriction
- ⊗ manual shutoff valve
- P pressure gauge
- dP differential P-gauge
- F flow meter
- ⊙ pump
- ⊙ turbomolecular pump
- ⊗ change-over-valve
- M pneumatic piston
- O-ring sliding seal
- ⊗ flow control valve
- 0.2μm filter
- 80 Dry ice water trap

490

**Figure 2.** Schematic depiction of the flow-stabilizing MS inlet system. Dashed orange arrows highlighted important control pathways and letters A-F-E in blue circles label the main sections of the inlet system. Red double arrows indicate manual switching option in the inlet system. Sample or standard Gas can either be delivered from samples in-high-pressure cylinders (A) or locally pumped ambient air (B). The flow can be measured by two Omron flow meters before entry into the pressure stabilization chamber (C). Pistons (DB) alternately move fine metal tubing in the pressure stabilization chamber, pushing

495

either the sample or standard gas stream deeper into the stabilization chamber where the gas will be picked up by a single capillary leading to the MS. A sliding seal is made using lubricated O-rings between 1/8" and 1/16" OD tubing at the entry to the pressure-stabilized chamber. This ensures sufficient rigidity and protects the fine metal tubing inside The chamber is exhausted to a vacuum system and the pressure is monitored and controlled by a differential pressure gauge combined with an automatic MKS flow control valve. The stainless-steel getter oven (~~ED~~) has an inner diameter of 1/2" and is filled with 10–12 g of titanium sponge. 2µm-filters prevent particles from contaminating the MS and gas delivery system. In case of an anomalous pressure change in the MS or when venting the getter oven, the getter oven can be isolated from the pressure-stabilization chamber with a change-over-valve controlled directly by the MS software. The entire inlet vacuum system is backed by a diaphragm vacuum pump and a turbomolecular pump (~~FE~~). A manual shutoff-valve can isolate the getter oven from the MS.

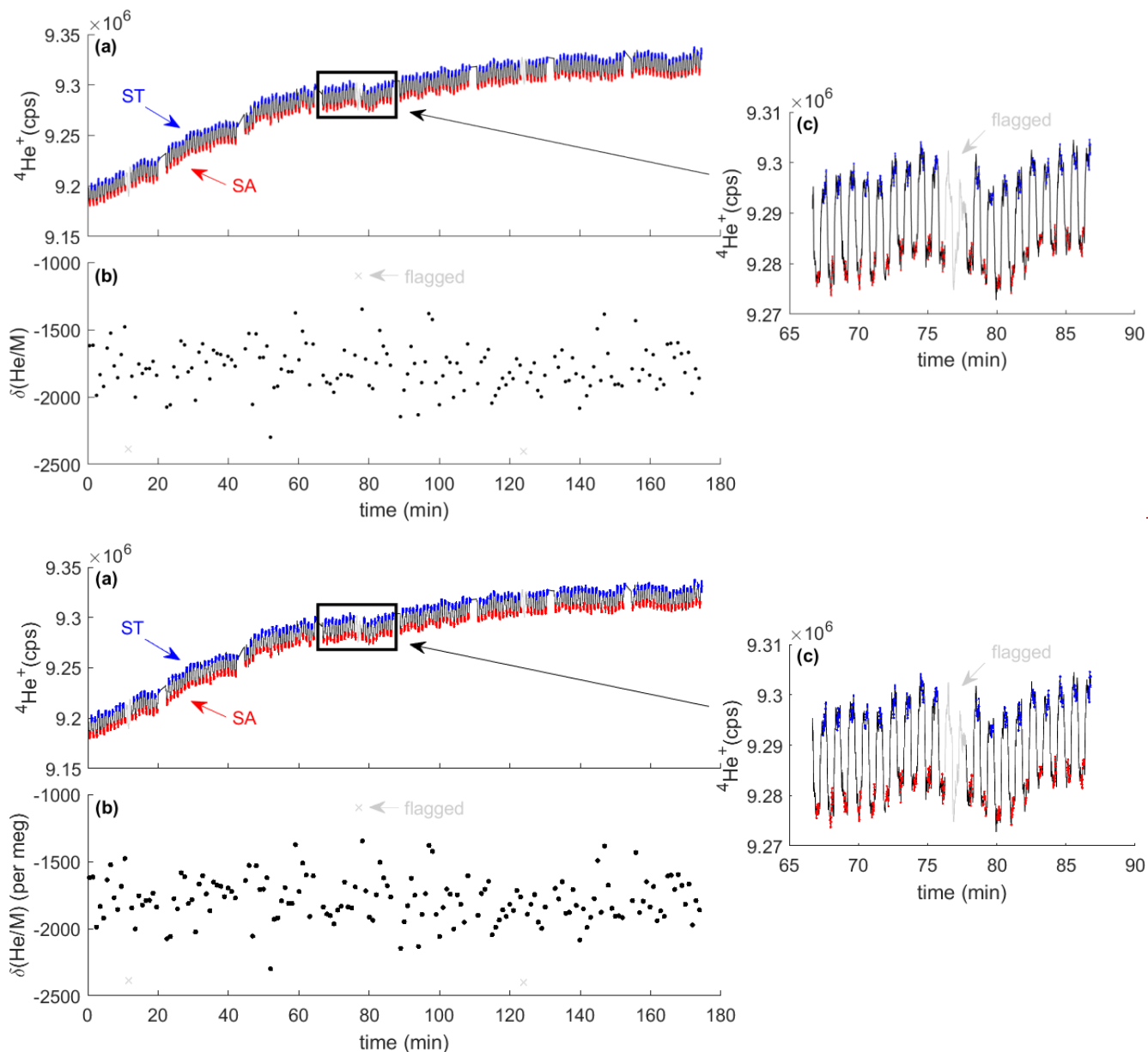


**Figure 3.** Typical analysis results from the measurement of two high pressure cylinders. The MS monitors the  ${}^4\text{He}^+$ -ion beam during switching between sample (SA) and standard (ST) gas (a). Red and blue shaded data points highlight the periods used for integration and calculation of the delta value (b). They are separated by idle times (black lines) to allow complete flushout after switching. Data are quality controlled and flagged periods are shown in grey. Inset (c) shows one block of 20 sample-standard comparisons including one cycled that was flagged as an outlier.

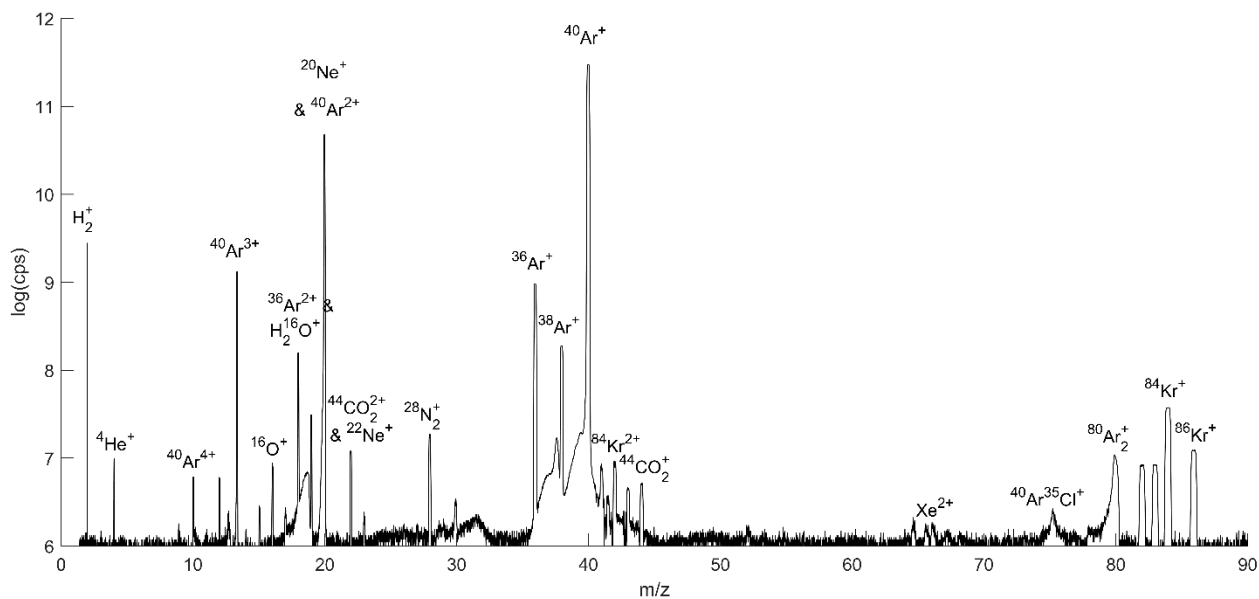


**Figure 4.** Mass scan of ambient air. Ion beam intensity is shown as the logarithm of the ions counted per second, and select ion species are labeled.

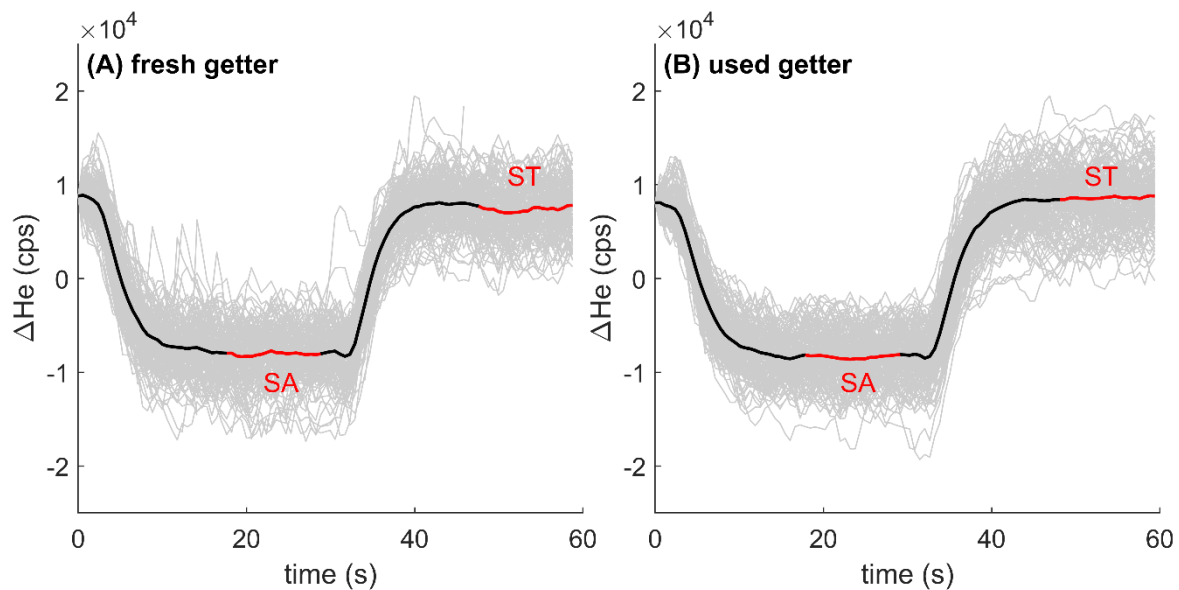


**Figure 5.** Stack of  $^4\text{He}$  ion count difference ( $10^4$  counts per second, cps) when switching between the same standard (ST) and sample (SA) gas stream using fresh titanium sponge (A) and nearly depleted getter material (B). Grey lines show individual records forced to align at time equals zero, and the thick black line shows the average of all stacked switching events. The analysis cycle consists of (i) switching to SA with an idle time of  $\sim 18$  seconds, (ii) a  $\sim 12$  second integration of ions from SA, (iii) switching back to ST, again with a  $\sim 18$  second idle time, and finally (iiii) a  $\sim 12$  second integration of ST.

520

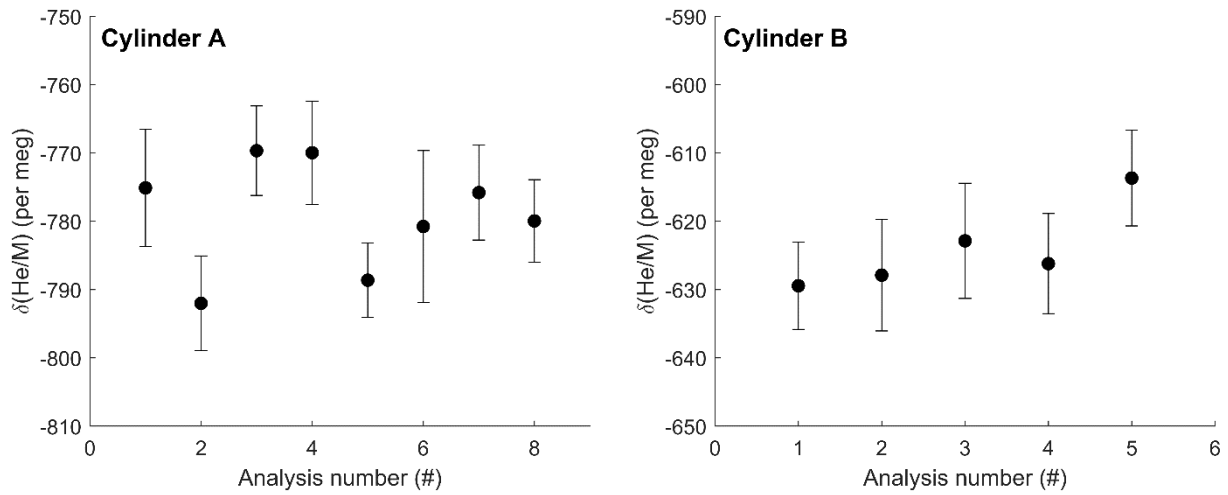


**Figure 6.** Repeat  $\delta(\text{He/M})$  measurement analysis of two high-pressure cylinders against ambient La Jolla air collected in 2019. Each data point shown is the average of at least 300 individual 12-sec measurements with  $1\sigma$  error bars representing the standard error of each measurement. Repeat analysis show a standard deviation of 8.1 and 6.3 per meg ( $1\sigma$ ) for cylinder A and cylinder B respectively. Analysis 6 for cylinder A was shorter resulting in a larger uncertainty for that measurement. Data are not corrected for zero enrichment effects discussed in the text.

525

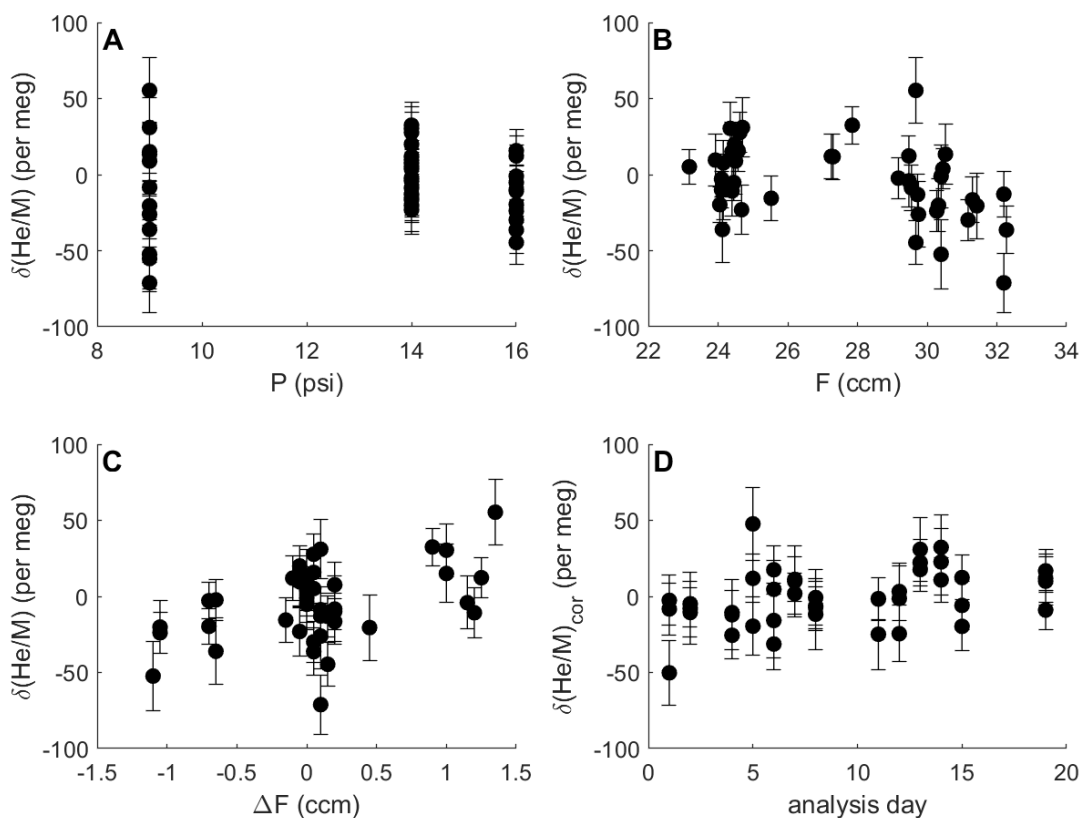


**Figure 7.** Difference in  $\delta(\text{He}/\text{M})$  between two identical gas streams (i.e., the zero enrichment) measured repeatedly under different conditions over 1.5–3h. Error bars show  $1\sigma$  uncertainty (internal precision). Measurements were made at different pressure levels (a), with slightly varying gas flows to the stabilization chamber (b), and imbalances in flow between SA and ST side (c). The same shared capillary was used for all analysis. Therefore, the pressure in the stabilization chamber controls the intensity of the ion beam and the internal precision of the analysis, illustrated by the greater scatter of observations at 9 psi (62.1 kPa). Delta values shown in (d) were corrected for the influence of pressure, mean flow, and flow imbalance according to coefficients found by multiple linear regression (see text). For a pressure of 14 psi (96.5 kPa), corrected delta values generally show scatter as expected from shot-noise behavior and corrected delta values are stable over time.

## 12 Tables and Table Captions

**Table 1.** Processes contributing to variations in the tropospheric and stratospheric  $^4\text{He}/\text{N}_2$  ratio.

Process	$^4\text{He}$ flux ( $10^7 \text{ mol y}^{-1}$ )	Tropospheric $\delta(^4\text{He}/\text{N}_2)$ trend <sup>1</sup> (per meg $\text{y}^{-1}$ )	Stratospheric $\delta(^4\text{He}/\text{N}_2)$ trend <sup>1</sup> (per meg $\text{y}^{-1}$ )	Tropospheric $\delta(^4\text{He}/\text{N}_2)$ anomaly (per meg)	Reference <sup>2</sup>
<b>Long-term trend</b>					
(1) Crustal degassing and volcanism	24.0–50.7	0.26–0.55			(a)
(2) Loss to space	53.3–106.8	–0.58–1.15			(a,b)
(3) Non-terrestrial sources	insignificant	–			(a)
(4) Global Ocean warming <sup>3</sup>	1.3	–0.16			
(5) Fossil fuel extraction <sup>4</sup>	3189–12755 13000±7000 34000	34–138 140±76 367			(c) (d) (e)
(6) BDC acceleration <sup>5</sup>		0.5	–15		
<b>Observational limits on decadal trends<sup>6</sup></b>					
		–1.4±44.5			(f)
		9.5±32.7			(g)
		–2±23.8			(h)
<b>Seasonal and interannual variability</b>					
Seasonal cycle of global ocean heat <sup>7</sup>				3–9	
Strat. circ. & STE variability <sup>8</sup>		±6	±375		
<b>Interhemispheric difference<sup>9</sup></b>					
				<30	

<sup>1</sup>  $\delta(^4\text{He}/\text{N}_2)$  trends are calculated using first column and assuming total atmospheric  $^4\text{He} = 9.268 \text{ e} + 14 \text{ mol}$ .  $\text{N}_2$  changes are generally neglected except for ocean degassing. Tropospheric trends are globally uniform because the troposphere is well mixed. Stratospheric trend estimates are given for 35km in the mid-latitude Northern Hemisphere.

<sup>2</sup> (a) Torgersen (1989)

(d) Pierson-Wickmann et al. (2001)

(g) Mabry et al. (2015)

–(b) Koekarts (1973)

(e) Sano et al. (2013)

(h) Boucher et al. (2018e)

–(c) Oliver et al. (1984)

(f) Lupton and Evans (2013)

<sup>3</sup> calculated from  $^4\text{He}$  and  $\text{N}_2$  solubility changes (Hamme and Emerson, 2004; Weiss, 1971) for an ocean heat content trend of  $10 \text{ ZJ y}^{-1}$  at a mean water temperature of  $10^\circ\text{C}$ .

<sup>4</sup> (c) includes natural gas, coal and uranium, (d) and (e) include natural gas, petroleum and coal.

<sup>5</sup>  $\delta(^4\text{He}/\text{N}_2)$  rescaled from  $\delta(\text{Ar}/\text{N}_2)$  assuming 7.5x greater gravitational separation. The secular  $\delta(\text{Ar}/\text{N}_2)$  trend was simulated in the SOCRATES model for an accelerating BDC scenario ( $+4\% \text{ dec}^{-1}$ ) by Ishidoya et al. (2020).  $\delta(^4\text{He}/\text{N}_2)$  trend is adjusted to reflect a more plausible BDC acceleration of  $+2\% \text{ dec}^{-1}$ .

<sup>6</sup> observed  $^3\text{He}/^4\text{He}$  trends are translated to  $^4\text{He}$  trends assuming  $^3\text{He}/^4\text{He} = 3\text{e}-8$  in fossil fuel associated helium.

<sup>7</sup> scaled from seasonal  $\delta(\text{Ar}/\text{N}_2)$  changes of 5–15 per meg (Keeling et al., 2004) using solubility-temperature dependency of He,  $\text{N}_2$  and Ar in a  $10^\circ\text{C}$  warm surface ocean (Hamme and Emerson, 2004; Weiss, 1971).

<sup>8</sup> Tropospheric and stratospheric  $\delta(^4\text{He}/\text{N}_2)$  rescaled from  $\delta(\text{Ar}/\text{N}_2)$ . Ishidoya et al. (2020) report a  $\pm 0.4$  and  $\pm 25$  per meg  $\delta(\text{Ar}/\text{N}_2)$  change in troposphere and stratosphere in the SOCRATES model for a sinusoidal  $\pm 5\%$  change in BDC strength over 3 years.

<sup>9</sup> Assuming that industrial He release is confined to the Northern Hemisphere and assuming an annual  $\delta(^4\text{He}/\text{N}_2)$  increase of  $\sim 30$  per meg (consistent with the current observational error) yields an interhemispheric  $\delta(^4\text{He}/\text{N}_2)$  difference  $< 30$  per meg. Differences in STE of He between the hemispheres are neglected here but could be important.

Process	$^4\text{He}$ flux ( $10^7$ mol $\text{y}^{-1}$ )	$\delta(^4\text{He}/\text{N}_2)$ trend <sup>1</sup> (per meg $\text{y}^{-1}$ )	$\delta(^4\text{He}/\text{N}_2)$ anomaly (per meg)	References
<i>Long-term tropospheric changes</i>				
(1) Crustal degassing and volcanism	24.0–50.7	0.26–0.55		(Torgersen, 1989)
(2) Loss to space	53.3–106.8	-0.58–-1.15		(Kockarts, 1973; Torgersen, 1989)
(3) Non-terrestrial sources	insignificant	-		(Torgersen, 1989)
(4) Global Ocean warming <sup>2</sup>	1.3	-0.16		
(5) Fossil fuel extraction <sup>3</sup>	3189–12755 13000±7000 34000	34–138 140±76 367		(Oliver et al., 1984) (Pierson-Wickmann et al., 2001) (Sano et al., 2013)
(6) BDC acceleration <sup>4</sup>		0.5		
<i>Long-term stratospheric changes</i>				
BDC acceleration <sup>4</sup>		-15		
<i>Observational constraints on tropospheric trends</i> <sup>5</sup>		-1.4±44.5 9.5±32.7 -2±23.8		(Lupton and Evans, 2013) (Mabry et al., 2015) (Boucher et al., 2018c)
<i>Short-term and spatial variability</i>				
Seasonal cycle of global ocean heat <sup>6</sup>			±1.5–4.5	
Strat. circ. & STE variability signal <sup>7</sup>				
-troposphere			±3	
-stratosphere			±187.5	
Interhemispheric difference <sup>9</sup>			<30	

<sup>1</sup>  $\delta(^4\text{He}/\text{N}_2)$  trends are calculated using first column and assuming total atmospheric  $^4\text{He} = 9.268 \times 10^{14}$  mol.  $\text{N}_2$  changes are generally neglected except for ocean degassing. Tropospheric trends are globally uniform because the troposphere is well mixed. Stratospheric trend estimates are given for 35km in the mid latitude Northern Hemisphere.

<sup>2</sup> calculated from  $^4\text{He}$  and  $\text{N}_2$  solubility changes (Hamme and Emerson, 2004; Weiss, 1971) for an ocean heat content trend of  $10\text{ZJ y}^{-1}$  at a mean water temperature of  $10^\circ\text{C}$ .

<sup>3</sup> (i) includes natural gas, coal and uranium, (ii) and (iii) include natural gas, petroleum and coal.

<sup>4</sup>  $\delta(^4\text{He}/\text{N}_2)$  rescaled from  $\delta(\text{Ar}/\text{N}_2)$  assuming 7.5x greater gravitational separation. The secular  $\delta(\text{Ar}/\text{N}_2)$  trend was simulated in the SOCRATES model for an accelerating BDC scenario ( $+4\% \text{ dec}^{-1}$ ) by Ishidoya et al. (2020).  $\delta(^4\text{He}/\text{N}_2)$  trend is adjusted to reflect a more plausible BDC acceleration of  $+2\% \text{ dec}^{-1}$ .

<sup>5</sup> observed  $^3\text{He}/^4\text{He}$  trends are translated to  $^4\text{He}/\text{N}_2$  trends assuming  $^3\text{He}/^4\text{He} = 3 \times 10^{-8}$  for fossil fuel associated helium. (Sano et al., 2013).

<sup>6</sup> scaled from seasonal  $\delta(\text{Ar}/\text{N}_2)$  changes of 5-15 per meg (Keeling et al., 2004) using solubility-temperature dependency of He,  $\text{N}_2$  and Ar in a  $10^\circ\text{C}$  warm surface ocean (Hamme and Emerson, 2004; Weiss, 1971).

<sup>7</sup> Tropospheric and stratospheric  $\delta(^4\text{He}/\text{N}_2)$  rescaled from  $\delta(\text{Ar}/\text{N}_2)$ . Ishidoya et al. (2020) report a  $\pm 0.4$  and  $\pm 25$  per meg  $\delta(\text{Ar}/\text{N}_2)$  change in troposphere and stratosphere in the SOCRATES model for a sinusoidal  $\pm 5\%$  change in BDC strength over 3 years.

<sup>8</sup> Assuming that industrial He release is confined to the Northern Hemisphere and assuming an annual  $\delta(^4\text{He}/\text{N}_2)$  increase of  $\sim 30$  per meg (consistent with the current observational error) yields an interhemispheric  $\delta(^4\text{He}/\text{N}_2)$  difference  $< 30$  per meg. Differences in STE of He between the hemispheres are neglected here but could be important.

**Table 2.** Summary of observed ion beams in Figure 4. Relative ion beam intensities on MAT253 are calculated from the scan with identical source tuning. Xe isotope beams were not observed but scaled from previous observations in the lab.

m/z	Dominant ions	Ion beam intensity (cps)*	ion beam intensity relative to He <sup>+</sup>
4	<sup>4</sup> He <sup>+</sup>	9.70E+06	1
20	<sup>20</sup> Ne <sup>+</sup> , <sup>40</sup> Ar <sup>2+</sup>	4.78E+10	4916.1
22	<sup>22</sup> Ne <sup>+</sup> , <sup>44</sup> CO <sub>2</sub> <sup>2+</sup>	1.22E+07	1.25
36	<sup>36</sup> Ar <sup>+</sup>	9.55E+08	98.26
38	<sup>38</sup> Ar <sup>+</sup>	1.89E+08	19.44
40	<sup>40</sup> Ar <sup>+</sup>	2.98E+11	30660
82	<sup>82</sup> Kr <sup>+</sup>	8.50E+06	0.87
83	<sup>83</sup> Kr <sup>+</sup>	8.40E+06	0.86
84	<sup>84</sup> Kr <sup>+</sup>	3.76E+07	3.87
86	<sup>86</sup> Kr <sup>+</sup>	1.22E+07	1.25
129*	<sup>129</sup> Xe <sup>+</sup>	2.60E+06	0.27
131*	<sup>131</sup> Xe <sup>+</sup>	2.10E+06	0.22
132*	<sup>132</sup> Xe <sup>+</sup>	2.70E+06	0.28
136*	<sup>136</sup> Xe <sup>+</sup>	9.00E+05	0.09

545 \*Xe isotopes were not measured directly here because of the limited dynamic range of the MAT 253 when set to measure He. Instead we report expected Xe ion beam intensities that were calculated using Kr ion beam intensities from this experiment and relative ion beam yields of scaled from previously analysis of Kr and Xe determined on a sperate MAT 253 in the lab assuming natural isotopic abundances.